

Review

Review of Thermal Management Strategies for Cylindrical Lithium-Ion Battery Packs

Mohammad Ahmadian-Elmi  and Peng Zhao * 

Department of Mechanical, Aerospace & Biomedical Engineering, UT Space Institute, University of Tennessee, Knoxville, TN 37388, USA; mahmadi4@utk.edu

* Correspondence: pzhao12@utk.edu

Abstract: This paper presents a comprehensive review of the thermal management strategies employed in cylindrical lithium-ion battery packs, with a focus on enhancing performance, safety, and lifespan. Effective thermal management is critical to retain battery cycle life and mitigate safety issues such as thermal runaway. This review covers four major thermal management techniques: air cooling, liquid cooling, phase-change materials (PCM), and hybrid methods. Air-cooling strategies are analyzed for their simplicity and cost-effectiveness, while liquid-cooling systems are explored for their superior heat dissipation capabilities. Phase-change materials, with their latent heat absorption and release properties, are evaluated as potential passive cooling solutions. Additionally, hybrid methods, such as combining two or more strategies, are discussed for their synergistic effects in achieving optimal thermal management. Each strategy is assessed in terms of its thermal performance, energy efficiency, cost implications, and applicability to cylindrical lithium-ion battery packs. The paper provides valuable insights into the strengths and limitations of each technique, offering a comprehensive guide for researchers, engineers, and policymakers in the field of energy storage. The findings contribute to the ongoing efforts to develop efficient and sustainable thermal management solutions for cylindrical lithium-ion battery packs in various applications.

Keywords: lithium-ion batteries; cylindrical cells; thermal management; air cooling; liquid cooling; phase-change material; hybrid cooling



Citation: Ahmadian-Elmi, M.; Zhao, P. Review of Thermal Management Strategies for Cylindrical Lithium-Ion Battery Packs. *Batteries* **2024**, *10*, 50. <https://doi.org/10.3390/batteries10020050>

Academic Editors: Carlos Ziebert, Xianglin Li, Chuanbo Yang and Prahit Dubey

Received: 15 December 2023
Revised: 20 January 2024
Accepted: 24 January 2024
Published: 28 January 2024



Copyright: © 2024 by the authors. Licensee MDPI, Basel, Switzerland. This article is an open access article distributed under the terms and conditions of the Creative Commons Attribution (CC BY) license (<https://creativecommons.org/licenses/by/4.0/>).

1. Introduction

Global warming is an urgent concern driven by the emission of greenhouse gases [1]. To combat this existential threat, there is an urgent need to shift our energy paradigm toward cleaner alternatives, particularly renewable energy sources like solar, wind, and hydropower. Unlike fossil fuels, these sources produce virtually no greenhouse gas emissions and are sustainable in the long run [2]. One of the key challenges with renewables, such as solar and wind, is their inherent variability and intermittency. Energy storage addresses this issue by capturing excess energy during periods of high production and releasing it at high demand or low supply conditions [3].

Energy storage systems can be categorized based on the type of energy stored into electrochemical, mechanical, electrical, chemical, and thermal energies [4]. Electrochemical energy storage refers to the process of storing electrical energy in the form of chemical energy and converting it back into electrical energy when needed. There are a few representative kinds of electrochemical energy storage systems: rechargeable batteries [5], electrochemical capacitors [6], and fuel and electrolysis cells [7]. Among these options, lithium-ion batteries (LIB) have become ubiquitous in modern electronics and electric vehicles because of their good energy density, relatively lightweight structure, and excellent rechargeability [8]. These batteries operate by the transfer of lithium ions between the electrodes, creating a current [9]. Various types of Li-ion cells, including cylindrical [10], prismatic [11], and pouch [12] designs, are accessible in the market for a wide range of applications.

Cylindrical lithium-ion batteries are a prevalent and versatile type of rechargeable power source with a distinctive tubular form. These batteries are widely utilized across numerous applications, including electronics, electric vehicles, and portable devices. Cylindrical lithium-ion battery cells comprise a rolled assembly, known as a jelly roll, which includes a cathode, an anode, a separator, and two current collectors for a unit layer. Common sizes, such as 18650 [13] and 21700 [14], have become industry standards, reflecting the popularity and reliability of cylindrical lithium-ion battery technology.

Similar to other chemical devices, battery performance is intrinsically influenced by temperature. As such, a suitable temperature range has to be maintained to guarantee performance and safety. Research suggests that to achieve optimal performance, it is advisable to limit the operation of LIBs to a specific temperature range, typically between 15 and 35 °C [15]. Temperature impacts batteries primarily through undesired chemical reactions and material degradations. Under low-temperature conditions, battery performance suffers from slow charge transfer and electrochemistry, as manifested by a substantial increase in internal resistance and a reduction in output power. High temperatures during the application of LIBs accelerate aging, negatively affecting performance and reducing overall lifespan. At even higher temperatures, thermal runaway may occur, where exothermic reactions are triggered among the battery materials [16], leading to subsequent fires and explosions.

In addition to temperature control, ensuring uniform temperature distribution within a battery has been a significant challenge for battery thermal management [17,18]. Inherent reversible entropic heat and irreversible polarization heat generations are associated with the normal operation of batteries. The escalating volumetric heat generation rate, associated with higher energy density and charge rates, necessitates an increased demand for cooling power to dissipate the accumulating battery heat. The situation is further complicated by the large number of cells included in a battery, many of which are subject to different thermal boundary conditions. The difference in thermal boundary conditions eventually leads to a temperature gradient within the battery pack, which further amplifies cell-to-cell variations among the pack in that cell; therefore, degradation strongly depends on temperature [19].

In fact, monitoring the thermal state of a battery itself is essential for maintaining it within safety limits and detecting potential thermal faults early on, preventing hazardous incidents like thermal runaways. Substantial efforts have been dedicated to implementing efficient onboard monitoring of battery thermal states. The primary method involves measuring battery temperature using devices like thermistors and thermocouples [20,21], through placing these temperature sensors on the battery surface to monitor its temperature during operations. Because of the restricted quantity of onboard temperature sensors and their incapacity to measure the internal temperature of the battery, estimating temperature becomes pivotal in overseeing the thermal condition of lithium-ion batteries (LIBs). Various metrics, including surface temperature, core temperature, bulk temperature, and temperature distribution, are employed as diverse measures for handling battery systems, each offering unique performance characteristics. Following that, existing techniques for estimating temperature can be classified into three categories: impedance/resistance-based estimation, thermal-model-based estimation, and data-driven estimation. Despite advancements at the cell level, challenges stemming from the intricate thermal dynamics of battery cells and packs, varying operating conditions, inadequate sensing of the pack, and limitations in the online applicability of current methodologies continue to hinder the effective monitoring of the thermal state at the pack or system level. Overcoming these challenges necessitates interdisciplinary efforts, including the application of advanced sensing technologies in the battery system, the derivation of high-fidelity control-oriented thermal models based on mathematical techniques, the utilization of state-of-the-art artificial intelligence (AI) technologies for precise and robust estimation, and the implementation of image processing methods to reconstruct temperature information [22].

The thermal conductivity of a cell plays a critical role in thermal management. The anisotropic layered structure of LIBs leads to a highly anisotropic thermal conductivity. In-plane heat conduction is primarily governed by the high thermal conductivity (k) of current collectors. The effective in-plane thermal conductivity falls within the range of 20 to 35 W/(m·K) [23,24]. Conversely, the effective cross-plane thermal conductivity is approximately 0.15–1.40 W/(m·K) [23]. This lower cross-plane k is a result of both the electrodes having low thermal conductivity and the presence of high thermal contact resistance between the layers [25]. In the particular case of cylindrical cells, the radial thermal conductivity is at least one order of magnitude lower compared to values in the longitudinal and azimuthal directions. A smart thermal management system should take advantage of the much faster in-plane heat conduction to remove heat more effectively.

To tackle these issues, lithium-ion batteries can be fitted with a battery management system (BMS) that oversees the regular functioning of the battery and optimizes its operation. Ensuring the safe functioning and extending the lifespan of a battery necessitates the presence of an efficient thermal management system. This paper presents a comprehensive review of the thermal management strategies employed in cylindrical lithium-ion battery packs. The review covers four major thermal management techniques: air cooling, liquid cooling, phase-change materials (PCM), and hybrid methods. Air-cooling strategies are analyzed for their simplicity and cost-effectiveness, while liquid-cooling systems are explored for their superior heat dissipation capabilities. Phase-change materials, with their latent heat absorption and release properties, are evaluated as potential passive cooling solutions. Additionally, hybrid methods, combining two or more strategies, are discussed for their synergistic effects in achieving optimal thermal management.

2. Battery Thermal Management Systems (BTMS)

Thermal management is a critical aspect of lithium-ion (Li-ion) battery packs to ensure their safe and efficient operation. The design of thermal management systems for cylindrical lithium-ion battery packs involves specific criteria to optimize performance and safety. First and foremost is the need for effective temperature control to maintain the battery within its optimal operating range, preventing overheating and potential safety hazards. Heat dissipation capability is equally vital, requiring the incorporation of materials with high thermal conductivity or other cooling mechanisms to transfer heat away from the battery cells efficiently. A well-designed thermal management system should also address temperature uniformity, ensuring that all cells within the battery pack experience consistent thermal conditions to avoid imbalances in performance and degradation. Additionally, the system should consider aspects such as thermal insulation to mitigate cold temperature effects and the prevention of thermal runaway events, emphasizing the importance of a comprehensive and multifaceted approach in managing the thermal challenges of lithium-ion batteries. Furthermore, achieving these criteria in a cost-effective manner is essential for the widespread adoption of lithium-ion batteries in various applications, including cost considerations of energy, material, and space. Therefore, an effective thermal management system for cylindrical lithium-ion battery packs must address these specific considerations to ensure both optimal performance and safety.

In addition to all the criteria that should be considered for the BTMS, two important features specific to cylindrical batteries should also be considered. The thermal conductivity of cylindrical cells differs in different directions, so the axial thermal conductivity is much more than the radial thermal conductivity. This feature makes the heat dissipation from the cell to the surrounding environment easier through an axial form of heat transfer. The second issue is the geometry of cylindrical packs. Due to the geometry of the cylindrical cells, their placement in the modules inevitably creates interstitial space among cells, which not only affects the volumetric energy density in the pack level but also adds extra constraints for heat removal and cooling system design.

BTMS for cylindrical lithium-ion battery packs can be broadly categorized into active and passive systems, each offering distinct approaches to address heat dissipation and

temperature control. Active systems incorporate mechanisms that actively remove heat from the battery pack, such as liquid cooling or forced air convection. Liquid-cooling systems use coolants to absorb and transfer heat away from the cylindrical cells, while air-cooling systems rely on fans or other methods to facilitate heat exchange. These systems are effective in regulating temperature and preventing overheating during high-demand scenarios. On the other hand, passive systems leverage natural heat dissipation methods, often incorporating materials with high thermal conductivity, like heat sinks or phase-change materials, to passively dissipate heat without the need for external mechanisms. The choice between active and passive systems depends on factors such as application, space constraints, and specific thermal management requirements, highlighting the need for a tailored approach to optimize the performance and safety of cylindrical lithium-ion battery packs. Commercial electric vehicles commonly employ air-cooling and liquid-cooling systems for the thermal management of lithium-ion batteries. For instance, vehicles like the Nissan Leaf and Mahindra e2o Plus utilize air cooling. On the other hand, models such as Tesla, Chevrolet Volt, Hyundai Kona, Ford Focus, and Jaguar I-Pace opt for liquid-cooling methods [26]. Recently, newer methods such as heat pipe [27–31], immersion cooling [32,33], and thermoelectric [34] have been used for the thermal management of lithium batteries. Figure 1 categorizes the different thermal management methods of cylindrical lithium-ion batteries.

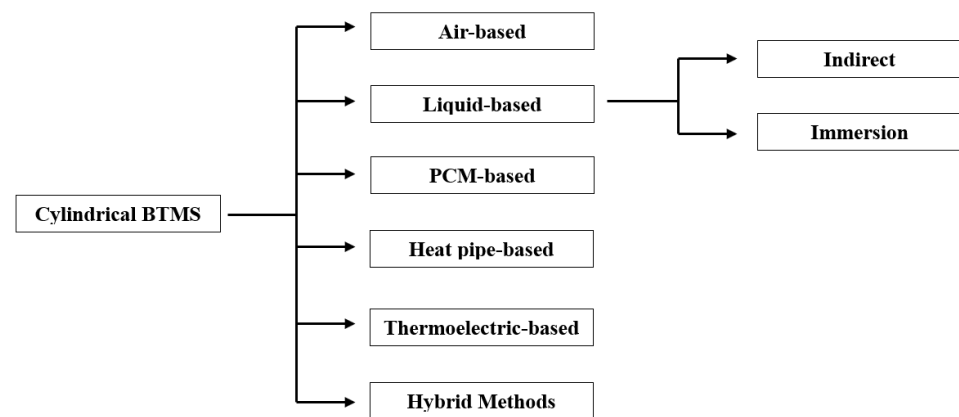


Figure 1. Classification of battery thermal management systems.

2.1. Air-Cooled BTMS

Air cooling is one of the most popular ways of heat dissipation in battery thermal storage systems (BTMS), due to its extensive advantages, such as its simple structural design, low cost, lightweight nature, ease of maintenance, long lifespan, simplicity in replacing a single cell, and little power consumption at a low battery discharge rate. In air-cooling systems, the battery is often equipped with cooling fins or other heat-dissipating structures that increase the effective surface area exposed to ambient air. As air flows over these structures, it carries away the heat, preventing the battery from overheating. Additional components, such as fans, may be incorporated to actively enhance air circulation and cooling efficiency.

Table A1 (presented in the Appendix A) summarizes the existing studies related to air-cooled cylindrical BTMS. This table classified the previous studies based on their method, battery type, number of cells, load, pack arrangement, airflow regime, airflow inlet, their main focus, and their achievements. Different battery types, including 18650, 21700, 26650, 32700, and 42110 were studied at various C-rates.

Researchers tried to study the air-cooling systems for different numbers of LIBs, from single cells to packs. Yang et al. [35] proposed a novel radiator featuring a surface structure inspired by bionics for each battery cell (Figure 2). The battery module comprises cells, fans, radiators, walls, and insulated frames. The cells are arranged in a parallel structure, with three rows along the battery axis. Insulated frames support and insulate

the cells, positioned between each row. Cooling air, propelled by the fan, enters each cell row and exits the battery module. Four radiators are placed in the gaps between four cells, with curved contact surfaces touching the outer cell surfaces. The curvature radius matches that of a cylindrical battery. Additionally, bionic surface structures with equilateral triangular cross-sections are affixed to the convex curved surface. In the air-cooled BTM system, cell-generated heat is conducted to the radiator through solid heat conduction. The cooling air then dissipates the heat, effectively controlling the battery module's temperature. To enhance cooling performance and minimize power consumption, they endeavored to optimize the radiator parameters, such as square plate thickness, and the height, shape, and length of the bionic surface structure. Their findings indicate that the novel radiator thickness and bionic surface structure height significantly reduce the maximum temperature values and temperature differences among the cells.

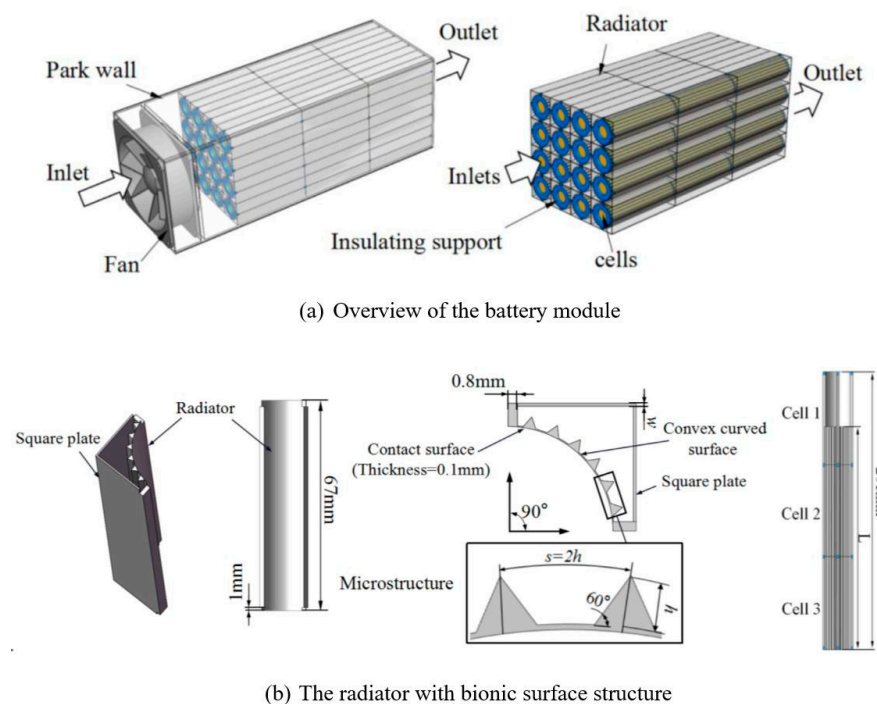


Figure 2. Scheme of the air-cooled battery management module with a bionic surface structure [35].

Designing a geometric structure for better air distribution has been one of the challenges of air-cooling systems. Yang et al. [10] explored the thermal characteristics of an air-cooled battery thermal management system specifically created for a cylindrical lithium-ion battery module featuring a honeycomb structure. They developed an air distribution plate (ADP) (refer to Figure 3) to improve temperature consistency within the battery module. Through the use of computational fluid dynamics (CFD), they conducted a numerical analysis of the cooling efficiency and airflow distribution. Modifying the width of the ADP channel was found to enhance the evenness of air distribution in the battery module spaces. Additionally, the utilization of a bionic heat sink demonstrates superior cooling effectiveness, significantly improving temperature consistency across the battery pack. Research has been conducted trying to provide geometric changes to improve air distribution. In another study, Zhou et al. [36] introduced an innovative cooling approach utilizing air distribution channels for cylindrical lithium-ion battery modules and conducted a numerical investigation (Figure 4). They examined the impact of orifice diameter, orifice rows, and inlet pressure. Their findings indicate that enlarging the orifice diameter and increasing the number of orifice rows contribute to lowering the maximum temperature and enhancing temperature uniformity. Importantly, this optimization comes with minimal additional power consumption.

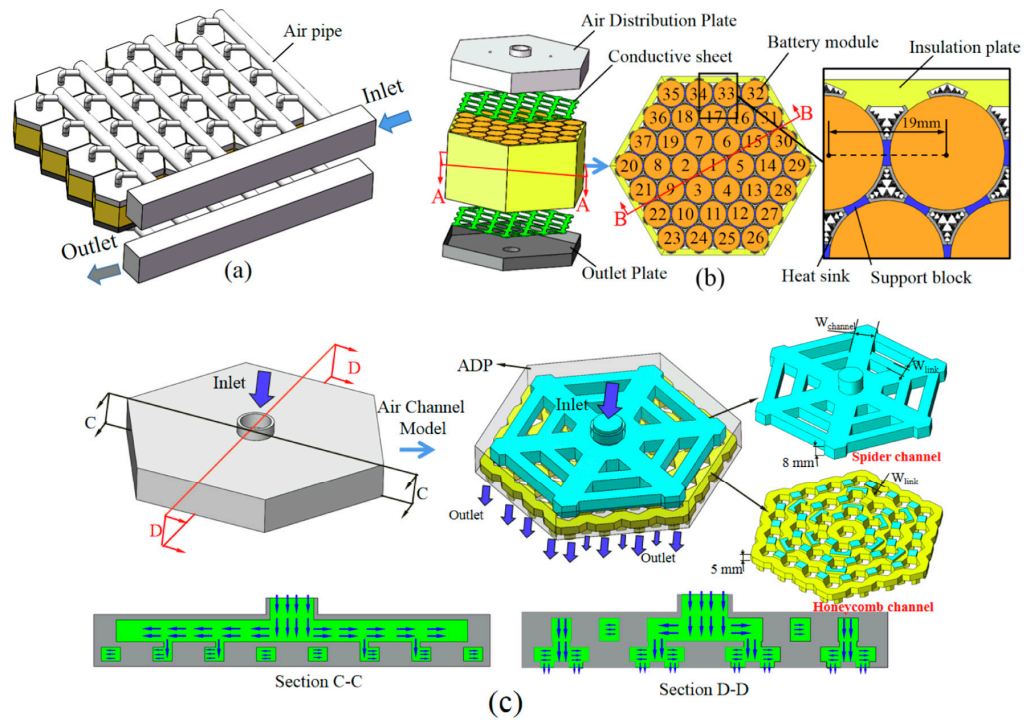


Figure 3. Structures and components of air-cooled BTMS: (a) battery pack, (b) battery module, and (c) air distribution plate [10].

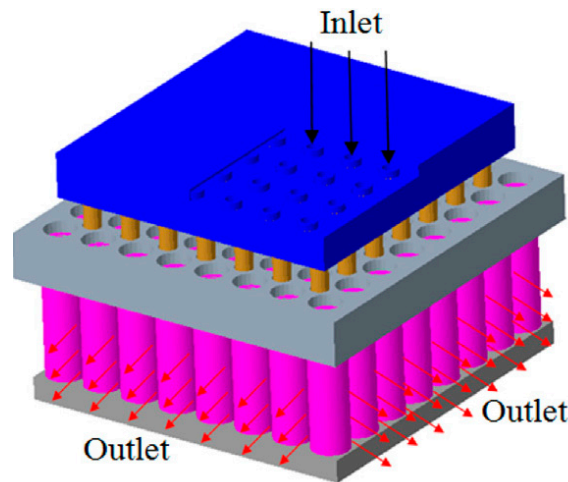


Figure 4. Schematic of the battery module using the air distribution pipe [36].

Changing the battery module structure can also be useful. Wang et al. [37] examined the heat efficiency of a battery module employing diverse cell arrangement structures such as rectangular, hexagonal, and circular configurations. The investigation also delved into optimizing air-cooling approaches by situating fans at different positions inside the battery module to enhance temperature uniformity. The research delved into factors influencing cooling capability based on simulations conducted using three-dimensional computational fluid dynamics (CFD). Heat generation rates were determined through thermal insulation experiments, and a lumped model was applied for individual cells. The findings revealed that placing the fan at the upper part of the battery module resulted in the most effective cooling performance, regardless of the structure. Among the structures tested, the 5 by 5 cubic arrangement demonstrated the best balance between cooling capability and cost. Meanwhile, the hexagonal structure with 19 cells was identified as the most favorable option for maximizing space utilization and ensuring effective cooling.

To enhance the cooling system's performance via geometric alterations, researchers designed jacket fins for each cell. Kummitha [38] introduced an innovative approach to achieve consistent temperature distribution within a battery module and reduce the maximum temperature reached by the battery cells. The novel module design incorporates cell holders at varying heights, serving as trays to support the battery cells and functioning as fins to enhance uniform temperature distribution. Comparative analyses were conducted on the base and new battery modules under different discharge conditions while maintaining consistent boundary conditions and physical parameters. In their design, jacket fins were implemented to enhance heat dissipation from the battery surface, ensuring a uniform thermal distribution. The heat removal plate, constituting the cell holder's jacket, was constructed using lightweight aluminum. Both models were evaluated under various discharge conditions using plane contours and temperature profiles for each cell within the battery module.

Air mass flow rate and channel design have a great impact on the performance of the air-cooling system. Lu et al. [39] developed a three-dimensional numerical model and an analytical thermal resistance model for a battery pack arranged in a staggered fashion. This was done to investigate how cooling channel design and air supply strategy affect the cooling efficiency of the battery pack. Their findings indicated that a larger cooling channel size can reduce the highest temperature and enhance the cooling energy efficiency of the stagger-arranged battery pack, although at the expense of space utilization, which subsequently influences the power density of the battery pack. Considering factors such as peak temperature, space utilization, and energy effectiveness, the optimal cooling channel size was determined to be 1 mm for the 18650 lithium-ion battery. Ji et al. [40] devised a lithium-ion cylindrical battery module incorporating distinct cell distribution strategies to enhance uniformity. They created a three-dimensional model to examine and enhance the configuration of the battery module. Introducing variations in the separation among cells, particularly through an arithmetic ratio arrangement, proves to be an effective method for improving homogeneity in the battery module. Furthermore, the highest temperature variation within the battery module decreased with an increase in the initial spacing. Comparing the arithmetic ratio and geometric ratio arrangements, it was determined that the arithmetic ratio arrangement yields superior temperature and discharge uniformities for the battery module. While the location of cells reaching the maximum temperature in the module changes over discharge time, they appear in a consistent position regardless of the configuration and initial gap. The process of changing positions was observed to be slower in arrangements with larger initial spacing and arithmetic ratios.

Using high thermal conductivity materials for components like thermal interface materials improves heat transfer and dissipation. Kausthubharam et al. [41] introduced a battery thermal system incorporating a commercially available thermal interface material, and they conducted a comparative analysis with a conventional battery pack across various discharge rates. Their approach demonstrates a noteworthy 25% decrease in peak temperature compared to the standard configuration. Lee et al. [42] created 21700 lithium-ion battery modules equipped with thermal interface materials (TIM). Their research revealed that the parallel thermal conductivity of the TIM significantly influences the temperature uniformity across the battery module. Meanwhile, the vertical thermal conductivity is more closely linked to the maximum battery temperature and State of Health (SoH).

One recent technology to increase the performance of cooling systems is the use of reciprocating flow, which is particularly useful in reducing cell-to-cell variations subjected to dissimilar thermal boundary conditions. Mahamud et al. [43] examined a novel battery thermal management technique employing reciprocating airflow for cylindrical Li-ion cells (Figure 5). Their analysis was conducted through numerical simulations utilizing a two-dimensional computational fluid dynamics (CFD) model, a lumped-capacitance thermal model for battery cells, and a flow network model. The results demonstrated that a shorter reciprocating period correlated with lower cell temperature differences and reduced maximum cell temperatures, both in instantaneous and time-averaged scenarios.

The enhancements achieved through reciprocating flow were primarily attributed to the redistribution of heat and the disruption of boundary layers formed on the cells due to the periodic reversal of airflow.

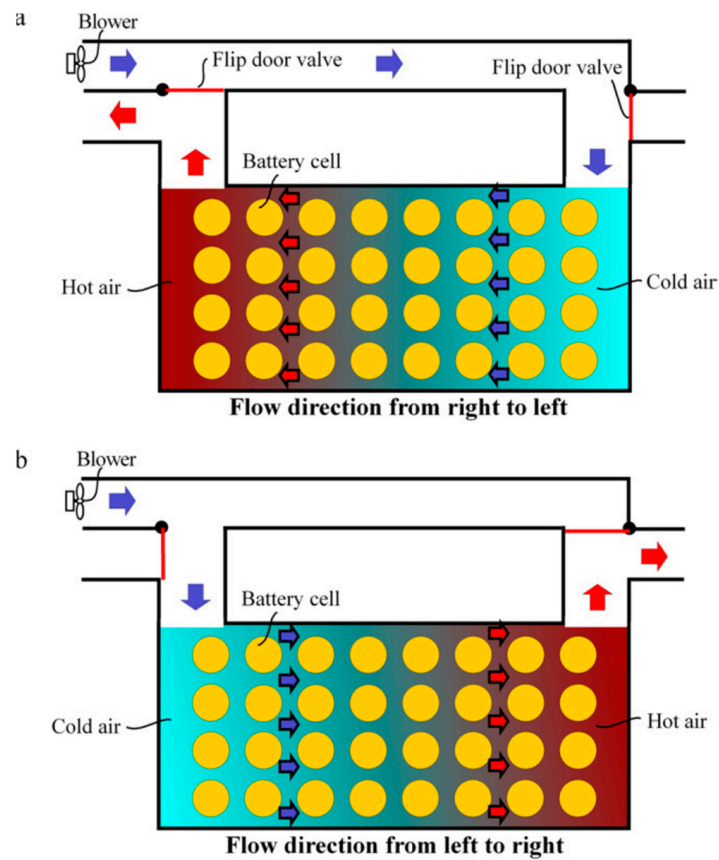


Figure 5. Schematic view of a battery system using a reciprocating airflow for battery thermal management. The flow directions are (a) from right to left and (b) from left to right [43].

Through advanced engineering and design strategies, researchers and engineers aim to optimize the airflow, cooling mechanisms, and overall thermal architecture of air-cooled lithium-ion battery systems. This includes the exploration of novel cooling materials, improved heat exchanger designs, and the development of smart thermal control systems. The goal is to achieve uniform temperature distribution within the battery pack, minimizing thermal gradients and preventing localized overheating. Wang et al. [44] introduced a multi-objective optimization approach using a BPNN-PSO method for an air-based BTMS. Initially, a database was established through CFD simulations before optimizing the design parameters. The optimization focused on channel spaces in the X-direction and air inlet velocity to enhance thermal performance and minimize energy consumption. Following the optimization of these parameters, further refinement of the BTMS was achieved by tuning the channel spaces in the Y-direction. The effectiveness of the BPNN-PSO method was validated against CFD simulation results under optimal conditions. The study revealed that the power consumption of the system, under optimal conditions, was reduced to 41.19% compared to the original system. Simulation analysis demonstrated the efficacy of the proposed multi-objective optimization method in significantly lowering the power consumption of the BTMS.

Precisely predicting temperature is a crucial challenge for enhancing battery performance and averting thermal runaway. The intricate nonlinear characteristics of heat generation and dissipation in lithium-ion batteries, coupled with susceptibility to external factors, make accurately forecasting battery temperature challenging. In recent years, the use of artificial neural networks (ANNs) has become widespread in various aspects of

lithium-ion batteries. Their distinct advantages in addressing highly nonlinear problems, including battery modeling, state of charge (SOC) estimation, residual useful life (RUL) prediction, and battery temperature prediction, have led to their extensive application in this field [45]. Li et al. [46] achieved the optimal design of battery thermal management systems through the implementation of a three-dimensional electro-thermal model combined with an artificial neural network (ANN) model. The three-dimensional electro-thermal model was utilized to compute the temperature distribution and was validated using previously gathered experimental data. Numerical case studies were conducted to train the proposed ANN model, revealing the correlation between geometric parameters, operating conditions, and cooling efficiency. Wang et al. [47] constructed a thermal model for lithium-ion batteries using an artificial neural network. Specifically, BP-NN, RBF-NN, and Elman-NN models were chosen to analyze the impact of network structures and modeling techniques on temperature prediction performance. The dataset for network training was acquired through a numerical model, and all three neural network models were configured with the same training parameters. The findings reveal that, under sample working condition testing, the RBF-NN model exhibits superior prediction accuracy and greater applicability, whereas the Elman-NN model performs less effectively.

According to the studies conducted in the air-cooling systems of LIBs, existing efforts to improve the performance of these systems can be classified into three aspects: (1) study and modify the geometry of these systems, such as channel dimensions, outlet and inlet positions, and changes in the number of air channels; (2) study of the airflow including change of flow direction, unidirectional and reciprocating flow, as well as inlet mass flow rate and velocity, type of flow regime (turbulent or laminar); (3) study battery working conditions such as different battery loadings and ambient air temperature.

In summary, air-cooled lithium-ion battery systems, despite their widespread use, present several drawbacks and limitations. One significant challenge is their limited cooling capacity, particularly in high-power applications where heat dissipation becomes crucial. These systems can be sensitive to ambient temperatures, making them less effective in extreme climates. The reliance on air cooling can lead to inconsistent temperature distribution within the battery pack, potentially resulting in hotspots that compromise overall performance. Additionally, air-cooled systems may lack the precision of more advanced liquid-cooling alternatives, and their design often adds bulk and weight to the battery pack. Noise generation from cooling fans and the potential for dust accumulation further contribute to the list of drawbacks. In high-temperature environments, air cooling may exhibit reduced efficiency, increasing the thermal stress of the cells. The maintenance requirements and energy consumption associated with air-cooled systems underscore the need to carefully consider alternative cooling solutions, especially in applications with demanding thermal conditions.

2.2. Liquid-Cooled BTMS

A liquid-based lithium-ion BTMS involves the use of a liquid, typically as a coolant or heat transfer medium, to regulate the temperature of the battery during operation. In this system, a liquid circulates through the battery pack, absorbing heat generated during the charging and discharging processes. The liquid absorbs the heat and then moves away from the heat source, where it can release the heat to the surroundings through a cooling mechanism. Table A2 (presented in Appendix A) summarizes the existing studies related to liquid-cooled cylindrical BTMS. This table classified the previous studies based on their method, battery type, number of cells, load, pack arrangement, airflow regime, flow inlet, their main focus, and their achievements.

Designing new systems according to the geometry of cylindrical cells is one of the researchers' priorities. Gao et al. [48] introduced an innovative design for a BTMS featuring gradient channels oriented along the flow direction (Figure 6). This design focused on the usefulness of achieving efficient heat transfer within the BTMS by maximizing the contact area between the solid components and the fluid. To address temperature gradient issues

along the flow direction, a liquid-cooled BTMS with a gradient channel-based design was proposed. The unique liquid-cooled structure comprised cooling tubes and multiple rows of cells, as illustrated in Figure 6. Cells were symmetrically positioned on both sides of the aluminum tube, facilitating a substantial heat dissipation area. The gradient cooling tube was segmented into two parts along the flow direction, with each large channel in the front corresponding to four small channels in the rear. This design aimed to increase the fluid–solid contact area in the rear segment. Through this gradient design, the heat generated in the cells is effectively transferred to the water, leading to a notable 69.40% enhancement in the temperature uniformity of the battery pack.

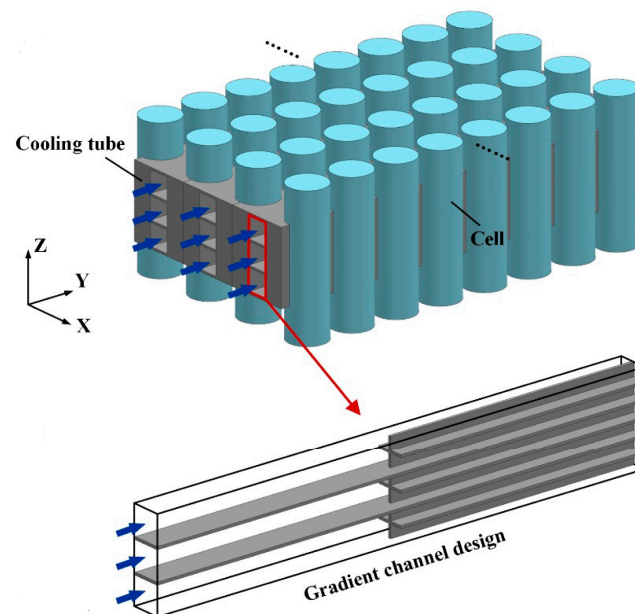


Figure 6. Schematics of a liquid-cooled BTMS with a gradient channel design [48].

Designing suitable channels for better heat dissipation is a key challenge of liquid-cooling systems. Kong et al. [49] explored the efficacy of two liquid-cooling configurations, namely the creation of mini-channel cylinders and a heat sink with channels for lithium-ion battery packs. The study utilized a 18650 lithium-ion cylindrical battery subjected to a 5 C discharge rate. The investigation delved into the impact of variables such as the number of channels, inlet/outlet positions, and mass flow rate on cooling efficiency, considering parameters like maximum temperature and temperature distribution. The findings indicated that augmenting the number of channels led to a reduction in the cell's maximum temperature, albeit with diminishing returns for each incremental increase. Additionally, the most optimal cooling performance was observed when the inlet was positioned closest to the battery end, resulting in enhanced heat dissipation under adiabatic conditions.

The widespread application of mini-channel cooling plates is observed in the liquid cooling of cylindrical cells. Li et al. [50] introduced an innovative liquid-cooling design incorporating mini-channel cold plates distributed vertically along the cells, utilizing water as the cooling medium. The researchers performed CFD simulations to assess the influence of different design parameters on the battery pack. Their specific emphasis was on evaluating the maximum temperature and the maximum temperature difference within the pack, liquid pressure drop, and overall pack weight. The authors highlighted that the incorporation of an aluminum cylindrical enclosure effectively addresses the issue of poor heat conduction through the battery material, significantly improving the cooling rate and temperature uniformity. Their findings indicated that the first design (battery pack with a cylindrical enclosure), featuring only three cooling plates, achieved thermal efficiency comparable to the second design (design without a cylindrical enclosure) with seven cooling

plates. Consequently, the cylindrical enclosure proves beneficial in reducing both weight and pumping power. Moreover, a square cross-sectional mini-channel is demonstrated with more effective heat dissipation and reduced flow resistance in comparison to circular and elliptical shapes. The study concluded that converging channels enhance heat removal and temperature uniformity but lead to increased pressure drop, while diverging channels reduce pressure drop at the expense of diminished thermal efficiency.

Researchers are trying to propose new structures for cooling systems. Xia et al. [51] devised an innovative heat sink for the cooling sleeve of a spindle, incorporating a novel network of fractal tree-like channels based on the constructal theory. Previous research indicated that such a heat sink with fractal tree-like channels offers inherent advantages in both heat transfer efficiency and pressure drop. The authors conducted a numerical analysis comparing the heat transfer and pressure drop characteristics of the fractal tree-like channels' heat sink with a conventional helical channel heat sink. The findings conclude that the fractal tree-like channels' heat sink exhibits a lower pressure drop, a more uniformly distributed temperature field, and a higher coefficient of performance compared to the traditional helical channel heat sink. Specifically, the coefficient of performance for the fractal net heat sink is more than twice that of the traditional helical net heat sink.

Parallel channels and serial channels are the conventional configurations of the liquid-cooling system. Wang et al. [52] introduced an innovative modular liquid-cooled system designed for batteries. They conducted numerical simulations and experiments to explore the impact of the mass flow rate of working fluid and cooling modes (parallel and serial) on the thermal characteristics of the battery module (Figure 7). The findings indicated that augmenting the flow rate within a defined range significantly lowers the maximum temperature and improves temperature uniformity in the battery module. However, surpassing a certain flow rate does not show a noticeable enhancement in cooling efficiency. Additionally, parallel cooling, compared to serial cooling, notably enhances the temperature consistency of the battery module.

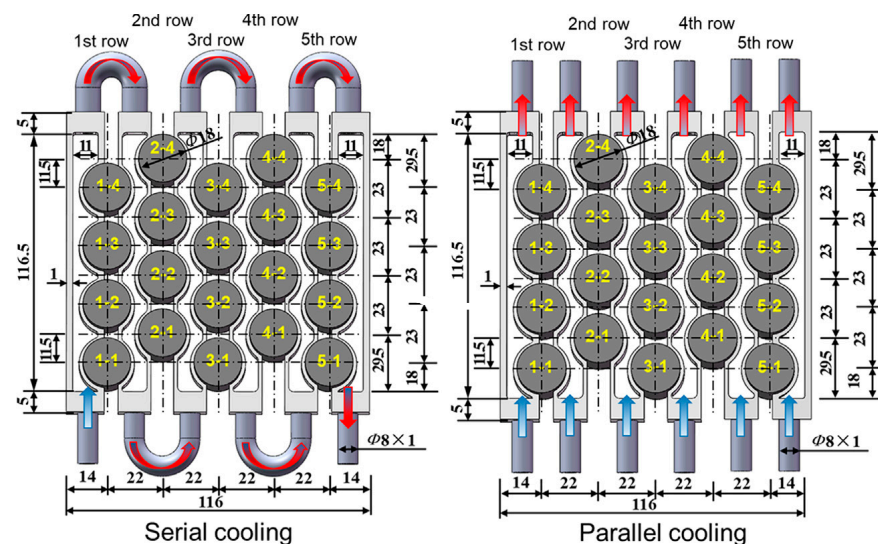


Figure 7. Schematic diagram of the serial cooling and parallel cooling [52].

The placement of the cold plate between the cells or their sides is also one of the issues that is taken into consideration and tested in different situations. Kim et al. [53] conducted experiments involving two battery packs equipped with distinct cold plates to assess and compare the cooling efficiencies of the battery thermal management system (BTMS). The study included an analysis of the internal heat generation within the battery modules, motivated by safety considerations. Figure 8 illustrates the two designed cold plates: Type I and Type II. In the case of Type I, four 18650 batteries were inserted into aluminum fins, with both ends of the fins in direct contact with the plate. Two cooling

channels were situated on the two edge sides of the cold plate. In Type II, an individual battery was positioned within a cylindrical aluminum fin, with the fins in contact with an aluminum cold plate. Four cooling channels were incorporated inside the aluminum cold plate, distributed among each battery row, facilitating the direct flow of water into the cooling channels. The fins were meticulously designed to match the outer diameter of the 18650 cells precisely. The findings indicated that Type II exhibited superior cooling efficiency compared to Type I at the same C-rate. Specifically, Type I demonstrated elevated battery temperatures at high C-rates, whereas Type II effectively maintained the battery temperature within the optimal range.

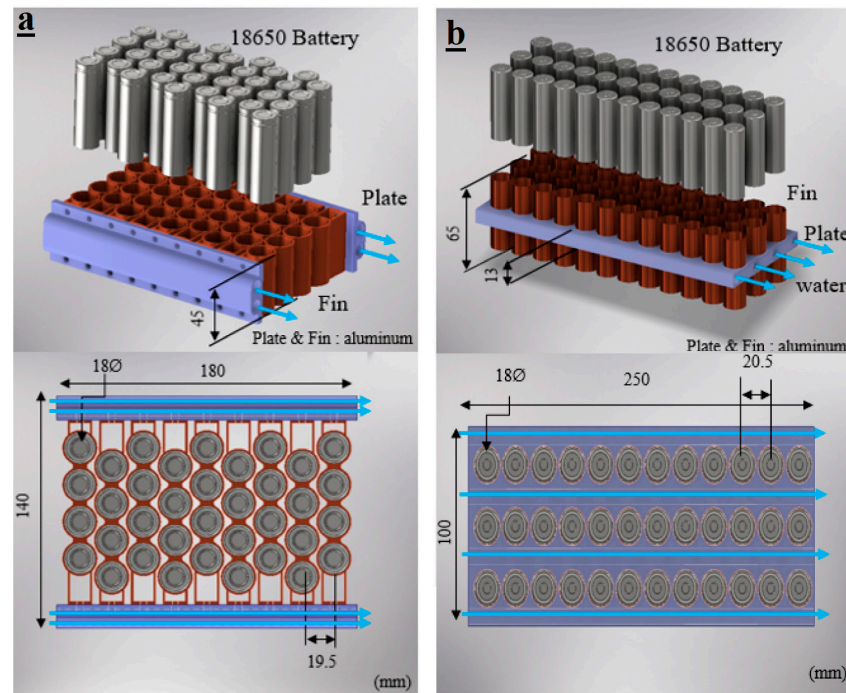


Figure 8. Battery module: (a) Type I and (b) Type II [53].

Some researchers suggest the implementation of cooling jackets to mitigate the undesired temperature increase and temperature variation in lithium-ion batteries. Sheng et al. [54] designed a liquid-cooling jacket with a cellular structure specifically for cylindrical lithium-ion batteries to mitigate undesired temperature increases and variations (Figure 9). In this approach, numerical investigations were conducted to analyze the impact of fluid flow, channel dimensions, and cooling medium on the thermal behavior of the battery cells. The results revealed that the interlaced flow directions within the developed cellular cooling jacket contributed to achieving a reduced temperature standard deviation and a more uniform thermal profile.

One of the most important design criteria of the cooling system is the ability to provide temperature uniformity in the module. Xu et al. [55] devised an innovative wrench-shaped design for a cylindrical battery module, aiming to specifically address the problem of temperature non-uniformity caused by a continuous rise in coolant temperature along the direction of the coolant flow (Figure 10). The effectiveness of the wrench-shaped cold plate was assessed through a comprehensive evaluation considering temperature rise control, preservation of temperature uniformity, lightweight design, and power consumption. The bifurcation structure incorporated into the wrench-shaped cold plate demonstrated a notably improved heat dissipation effect at the junction between the upstream and downstream segments.

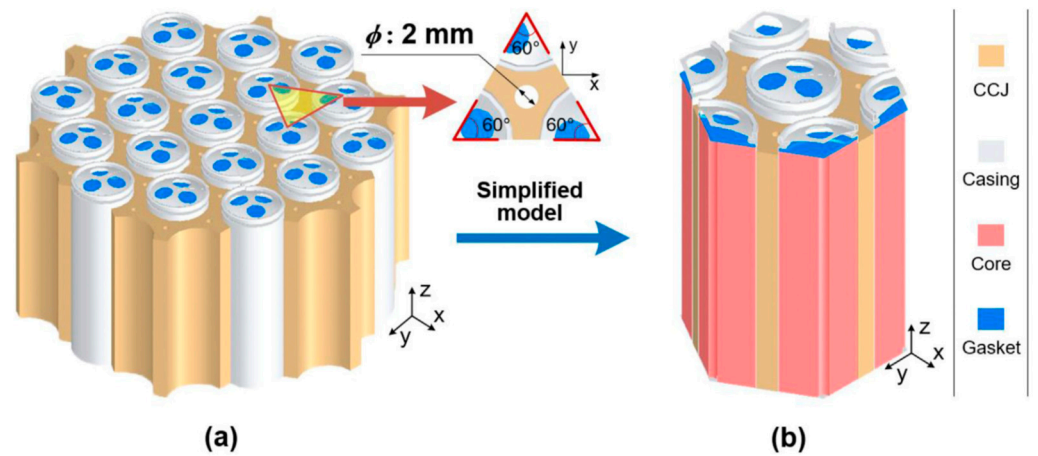


Figure 9. Power battery module. (a) Battery module consisting of multiple 21700 cells; (b) Simplified CAD model for the module [54].

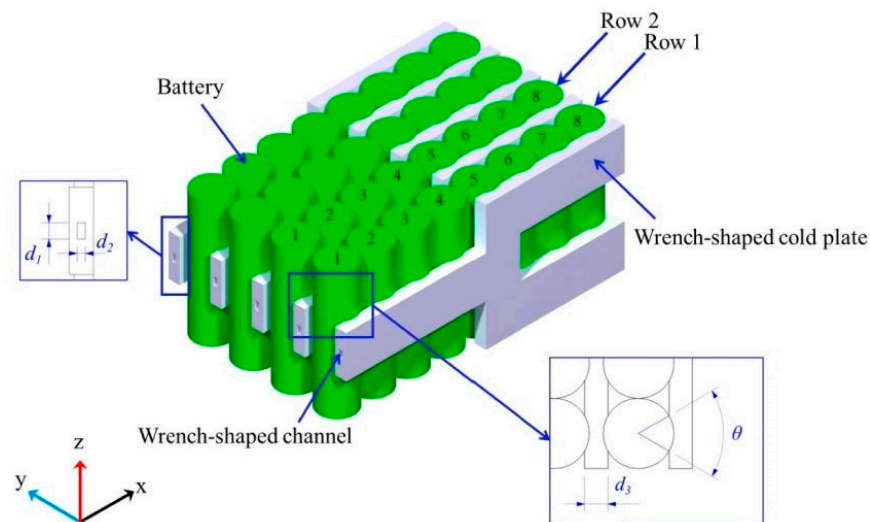
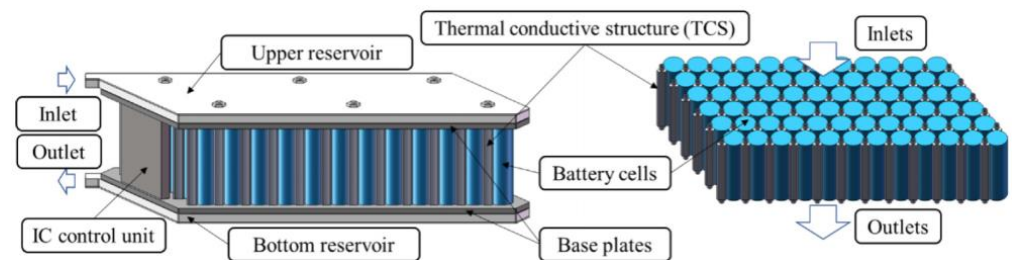


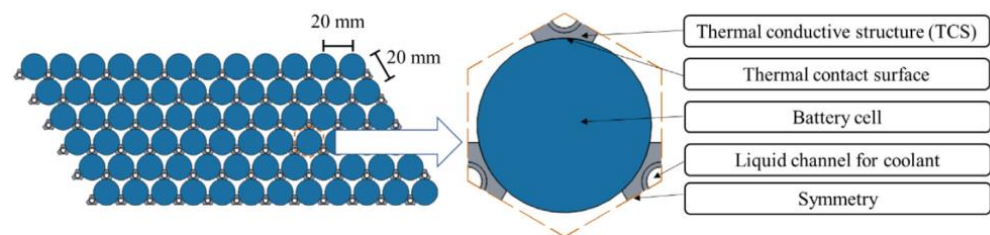
Figure 10. Schematic diagram of the liquid-cooling BTMS [55].

Minimizing the temperature differences poses a greater challenge compared to decreasing the maximum temperature and requires a novel structure for liquid channels. Liu et al. [56] designed an innovative liquid-cooling system that incorporates a vertical tube layout (VLT) along with a combination of gradually increased tube diameter. The research explored the influence of two tube configurations, the diameter of the tube, flow rate, gradient ratio flow velocity, and gradient-incremented tube diameter on the thermal efficiency of the system. The finding indicated that, within a defined range of flow velocities, the battery module featuring a vertical tube layout demonstrates superior performance compared to the horizontal configuration. Moreover, compared to a constant flow velocity and tube diameter, implementing a strategy involving either a gradient ratio flow velocity or a gradually increased tube diameter can reduce temperature differences in the battery, and combining both approaches can further improve temperature uniformity. Tete et al. [57] devised an innovative battery pack design that incorporates cylindrical casings for inserting batteries and utilizes a liquid-cooling medium circulated in its surroundings. Numerical simulations were conducted employing the finite volume method under various operating conditions, including scenarios with no cooling and with water cooling. The observations revealed that the highest heat accumulation occurred at the center of the battery pack. The maximum temperature increase was observed in the cells located at the core of the battery pack, as the coolant that reached this area had already warmed by absorbing heat from cells in the preceding rows.

A key feature that a BTMS desires is to be lightweight. A small, lightweight liquid-cooled BTMS was presented by Lai et al. [58] to manage the maximum temperature and temperature differential of a lithium-ion power battery pack. Their battery pack consists of base plates, liquid-cooled BTMS, an IC control unit, and 18650-type battery cells. Thermal conductive structures (TCSs), a bottom reservoir, and an upper reservoir make up the liquid-cooled BTMS. Engineered polymers are used to make the bottom reservoir and upper reservoir in order to save weight. The cells are arranged in a staggered pattern with a fixed gap between each one. The TCSs are placed inside the cell gaps for a compact size consideration, as seen in Figure 11. Three TCSs surround every cell. Each TCS has a circular liquid channel with a coolant setting in the middle. Each TCS is made with three curved contact surfaces in order to provide efficient thermal contact. By assessing the effects of inner diameter, contact surface height, and contact surface angle on temperature difference, they concluded that choice of inner diameter affects weights the most.



(a) Overview of the module and the contacts between the batteries and the TCSs



(b) Top view of the TCSs and the batteries

Figure 11. The scheme of the liquid-cooled battery management module [58].

Developing a compact cooling system for cylindrical LIB modules by effectively utilizing the spaces between the cylindrical batteries is a desired approach that will not further decrease the pack volumetric energy density. Shan et al. [59] introduced an innovative liquid-cooling BTMS featuring axially mounted cooling tubes inserted into the gaps between tightly assembled batteries, providing a compact and lightweight solution for cooling cylindrical battery modules. Their work considered the effects of different battery arrangements, leading to the proposed two designs for BTMS with axially mounted cooling tubes (Figure 12). In Design A, a staggered battery arrangement was implemented. The corresponding cooling tubes inserted between the batteries had the same height as the batteries and featured three curved contact surfaces to ensure effective heat contact. To achieve uniform heat dissipation, each battery was surrounded by three cooling tubes, covering half of the battery's side surface. In total, 65 tubes were inserted into the battery module. A circular coolant channel was positioned at the center of the cooling tube, allowing the coolant to flow axially from the top to the bottom of the batteries to dissipate the generated heat. In Design B, an aligned battery arrangement was employed. To adapt to the structural characteristics of the aligned battery module, the cooling tubes inserted between the batteries were designed with four curved contact surfaces, with a curvature radius identical to that of the battery. The height of the cooling tubes matched that of the

batteries. They observed that the cooling performance of the BTMS in Design B surpassed that of Design A. However, the BTMS in Design A incurred significantly lower weight and volume costs (0.13 kg and 1.09 L, respectively) compared to the BTMS in Design B (0.72 kg and 1.26 L, respectively), highlighting the superior lightweight and compact characteristics of Design A.

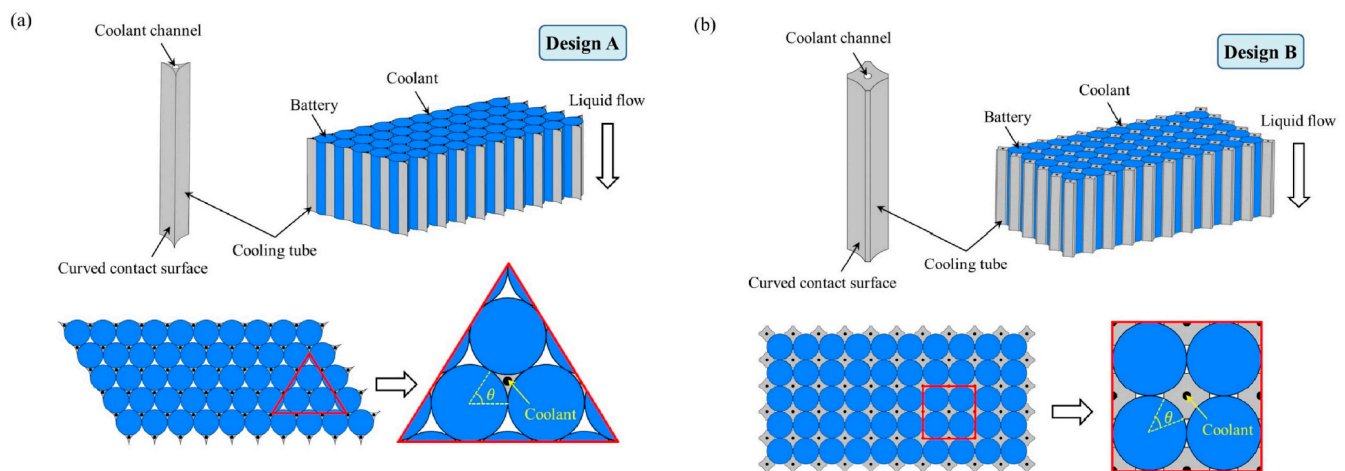


Figure 12. Schematic diagrams of the liquid-cooling battery module with axially mounted cooling tubes: (a) Design A with a staggered battery arrangement; (b) Design B with an aligned battery arrangement [59].

Pumping power in a BTMS refers to the energy required to circulate a cooling function through a system, and it is the energy consumed by the pump to overcome friction, pressure drops, and other resistances in the fluid circulation system. An efficient BTMS aims to strike a balance between effective heat dissipation and the energy required to circulate the cooling fluid, ensuring optimal performance and energy efficiency. Xiong et al. [60] developed a heat exchanger featuring a structure reminiscent of a spider web, leveraging the benefits associated with a large surface area, high convective heat transfer coefficient, and efficient fluid flow. This design effectively maintains the battery within the appropriate temperature range while minimizing power consumption. When compared to honeycomb-like and traditional helical structures with identical volume fractions and geometric parameters, heat exchangers utilizing the spider-web-like structure exhibit superior thermal and flow characteristics. Liang et al. [61] suggested a unitization-based BTMS solution, incorporating an innovative distributed water-cooling component to address the thermal management challenges of cylindrical LIB packs in EV applications. They aimed to strike a reasonable balance between system cooling performance, power consumption, and lightweight design.

To further facilitate heat transfer, nanofluids have emerged as a promising solution in liquid-cooling systems for BTMS. These nanofluids, consisting of a base fluid and suspended nanoscale particles, exhibit exceptional thermal conductivity, surpassing that of conventional coolants. When integrated into the liquid-cooling systems of LIBs, nanofluids enhance the efficiency of heat transfer, effectively mitigating issues related to overheating during high-power operations. Tousi et al. [62] developed an innovative indirect liquid-cooled BTMS for cooling a battery pack comprising 12 cells. The proposed schematic aimed to control the maximum temperature and thermal non-uniformity, particularly through the use of unidirectional flow. This method intentionally delays the fluid's exit from the channel, maximizing the fluid's cooling efficiency. The novel indirect liquid-cooling channel BTMS was designed to encompass all sides of the batteries, providing a large heat exchanger area to cool the heat generated from all the battery surfaces through heat conduction and dissipation by cooling DI-water and AgO nanofluid in the channel. The study revealed that the addition of AgO nanofluid into the channel significantly contributes to reducing the highest temperature and temperature non-uniformity in the battery pack. However,

this method comes with an increased pressure drop in the channel. Transitioning from DI-water to AgO 4% nanofluid results in a 10.1% decrease in the maximum temperature and a 23.95% decrease in the temperature difference values of the battery pack.

Alumina nanofluid is one of the most effective fluids used in liquid-cooling systems. Sarchami et al. [63] devised an innovative BTMS, which incorporates wavy/stair channel liquid cooling and a copper sheath. The wavy-type channel not only aligns with the geometry of LIBs but also offers a substantial contact surface. Additionally, the stair channel is specifically designed to reduce the temperature at the top section of the battery pack. The study revealed that incorporating alumina nanoparticles into the base fluid, i.e., DI-water, enhances the cooling efficiency of the battery pack. When transitioning from DI-water to a 2% volume fraction alumina nanofluid, the peak temperature during charge operation and temperature non-uniformity values decrease by 2.4 K and 0.26 K, respectively. Similarly, for discharge operation, these values were approximately 2.33 K and 0.54 K lower, respectively.

Similar to air cooling, the reciprocating motion in liquid-cooling systems for BTMS offers an effective approach to optimize heat dissipation. In such a system, the cooling fluid undergoes back-and-forth motion within the cooling channels, facilitating efficient heat transfer. This motion can be controlled and adjusted based on the specific thermal requirements of the battery and environmental conditions. The reciprocating flow helps prevent the formation of hotspots by ensuring uniform cooling across the battery cells. Zeng et al. [64] utilized a reciprocating-liquid-flow-based BTMS for cylindrical batteries to address these associated issues (Figure 13). They conducted a comparative analysis among unidirectional flow, cross-direction flow, and reciprocating flow to assess the efficacy of reciprocating flow. Their findings demonstrated that reciprocating flow outperformed both unidirectional and cross-directional flows. The researchers further investigated the impact of velocity and reciprocating period, identifying them as key factors which influenced reciprocating flow. They proposed a comprehensive criterion for BTMS performance, considering maximum temperature, temperature difference, temperature distribution coefficient, and energy consumption, aiming to optimize reciprocating flow. They achieved a significant reduction of 55.3% in temperature difference and a 15.6% decrease in energy consumption.

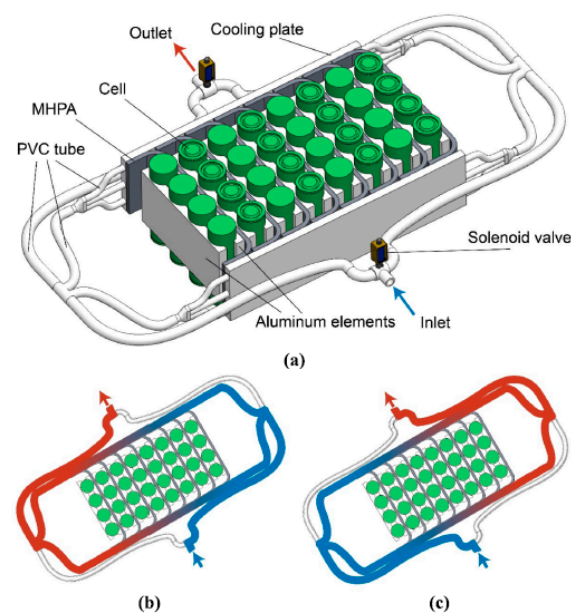


Figure 13. Geometric model of the BTMS with reciprocating flow. (a) Schematic diagram of the BTMS. (b,c) Diagram of reciprocating flow [64].

Optimization in liquid-cooling systems for lithium-ion batteries is critical to enhance battery performance, longevity, and safety. The optimization process involves a careful

consideration of factors such as coolant flow rate, heat exchanger design, and pump efficiency. Engineers strive to strike a balance, ensuring that the cooling system effectively dissipates heat from the battery cells while minimizing the associated energy consumption, known as pumping power. Ma et al. [65] suggested an optimization approach for cooling lithium-ion batteries using a triple-step nonlinear method. To overcome the current limitation where the coolant flow rate cannot be precisely aligned with the actual cooling requirements of batteries in thermal management systems, the researchers introduced a triple-step nonlinear approach. They developed a simplified thermal model for lithium-ion batteries employing liquid cooling. The model takes into account factors such as heat generation, heat dissipation mechanisms, and the heat balance equation of the batteries. Wang et al. [66] introduced a combined strategy that integrates single-factor analysis with orthogonal testing to streamline the optimization process for the liquid-cooling structure in extensive battery modules. They illustrated that the contact angle exerts the most substantial influence on cooling performance, while the channel number exhibits a minimal impact in large battery modules with elongated channels. Consequently, for large battery modules, several potential factor combinations are suggested, such as maintaining a fixed contact angle of approximately 70° . The appropriate values for inlet velocity and channel number can vary within the ranges of $0.2\text{--}0.5\text{ m}\cdot\text{s}^{-1}$ and $1\text{--}2$, respectively, depending on specific applications.

Researchers proposed a method to improve the heat transfer coefficient by introducing baffles into the micro-channels. Xie et al. [67] investigated a micro-channel liquid-cooling system for the EV battery modules. They developed a computational model that couples the heat transfer process from electrochemical–thermal predictions at the cell level to the overall calculation of the battery module. Numerical results demonstrated that the inclusion of baffles in the cooling micro-channels of the battery module could elevate the temperature gradient at the channel wall by enhancing flow mixing. As the height and number of baffles increase, a further improvement in heat transfer effects is achieved for the battery pack, albeit with an accompanying increase in the pressure required to drive the coolant flow.

Although liquid cooling for BTMS has considerable advantages, it has its drawbacks too. These systems can be complex and expensive due to additional components such as pumps and heat exchangers, leading to higher upfront costs and increased maintenance complexity. The risk of leaks poses a significant concern, which results in damage and safety hazards. The weight and size of liquid-cooling systems may be limited in applications where space and weight are critical factors. Compatibility issues during integration, potential energy consumption concerns, the risk of coolant freezing with volume change in cold environments, and environmental impacts further contribute to the considerations that must be weighed against the advantages of efficient heat dissipation.

2.3. PCM-Cooled and PCM-Fin BTMS

PCM (phase-change material) thermal management for LIBs involves the use of PCMs to regulate and control the temperature of the battery cells during various operational conditions. PCMs are substances that can absorb or release thermal energy during the process of changing phases, such as from solid to liquid or vice versa. PCMs with melting points ranging between 20 and $50\text{ }^\circ\text{C}$ are commonly employed in research, aligning with the operational temperatures of batteries. The key advantages of PCM usage are linked to their substantial latent heat and their role in temperature regulation. This facilitates the isothermal absorption of heat generated by cells when their temperature surpasses the melting point. Conversely, when the battery temperature is low, the PCM releases heat isothermally. A BTMS based on PCMs thus holds the potential to control battery packs effectively at desired operational temperatures. A PCM-based BTMS exhibits four distinct melting stages during operation. In the initial stage, battery temperature rises significantly with heat conduction dominating, storing heat as sensible heat. The temperature increase slows in the second stage, reaching an equilibrium in the third stage when natural convection and latent

heat energy storage offer robust cooling. The fourth stage sees the consumption of latent heat, and heat dissipation occurs through natural convection. Challenges in PCM-based BTMS are associated with the core PCM, characterized by low thermal conductivity, high volume change, low form stability, and flammability (organic PCM). Most PCMs exhibit low thermal conductivities between 0.2 and 0.4 W/(m·K), which are suboptimal for efficient heat transfer [68]. To address this, promising solutions involving creating heat conduction paths and incorporating thermally conductive materials such as porous materials and nano additives into PCMs have been explored. Porous materials absorb PCMs, forming heat conduction paths to enhance thermal conductivity. Nano additives significantly improve thermal conductivity with a minimal mass or volume ratio, although measures must be taken to preserve form stability [69]. Table A3 (presented in Appendix A) summarizes the existing studies related to PCM-cooled cylindrical BTMS. This table classified the previous studies based on their method, battery type, number of cells, load, PCM composite, melting point, thermal conductivity, main focus, and achievements.

PCM-based cooling systems are usually accompanied by fin structures. Fins are thin, extended surfaces that are added to heat transfer surfaces to enhance the efficiency of heat dissipation. The design of fins involves considerations such as length, thickness, spacing, and material properties, all of which impact the overall heat transfer performance. An optimized fin structure increases the surface area available for heat exchange, promotes better airflow, and ultimately improves the cooling efficiency of the system, helping to maintain optimal operating temperatures for the associated equipment. Najafi et al. [70] devised an optimal BTMS by integrating PCM, metal foam, and fins. They assessed the thermal performance under a discharge with a 3C current rate. According to their findings, the BTMS incorporating PCMs, metal foam, and fins exhibited a maximum reduction of 3 K in battery surface temperature compared to a system using pure PCMs. Additionally, this configuration demonstrated a maximum delay of approximately 470 s in the PCM melting process. The results from this optimized BTMS design revealed that the applied fins function as a network of heat sources, facilitating heat dispersion within the system. The use of metal foam contributed to a uniform distribution of heat between the battery and the surrounding environment. Moreover, the analysis of PCM melting indicated that the primary factor contributing to the delay in PCM melting was the integration of metal foam and fins within the BTMS.

Metal fins are favored for their straightforward structures and easy manufacturability, leading to their extensive application in the cooling of LIBs. Sun et al. [71] introduced innovative fin structures comprising longitudinal fins and cylindrical rings, and assessed the impact of various parameters, including the position and number of the cylindrical rings, the number of longitudinal fins, and the heat generation rate, on the thermal management effectiveness of the PCM–fin-based BTMS (Figure 14). Their BTMS configuration included a cylindrical battery, metal fins, PCM, and a nylon housing, with the battery positioned at the center of the cylindrical housing. Metal fins, incorporating a cylindrical ring and four longitudinal fins, enveloped the outer surface of the battery. The ring and fins matched the height of the battery, while the remaining housing sections were filled with paraffin wax. Their findings indicated that the proposed fin structures established a thermally conductive network within the PCM, facilitating the rapid transfer of heat generated in the battery to the PCM and significantly extending the battery's operational duration. Additionally, employing more than one ring increased the heat transfer area between the battery and the PCM but adversely affected the BTMS's thermal management performance due to an excessive reduction of PCMs within the system.

Observing the melting process of PCMs provides an effective means to analyze the thermal characteristics of PCM–fin systems. Chen et al. [72] tried to determine the optimal size of the battery compartment and the number of fins to minimize the maximum battery temperature during the discharge phase (Figure 15). In their investigation, a cylindrical battery was immersed in a chamber filled with a phase-change material (PCM), and several fins of equal length were affixed to the battery. The finding indicated that the battery, fitted

with 15 fins, had the most advantageous performance in terms of PCM melting at the onset of the cooling procedure. Around one-third of the cooling duration, the PCM reached its peak melting, measuring 26.16%. Additionally, throughout the entire cooling period, the battery with nine fins exhibited the lowest maximum temperature and the highest volume fraction of liquid PCMs. Beyond this point, an increase in the number of fins led to an elevation in battery temperature.

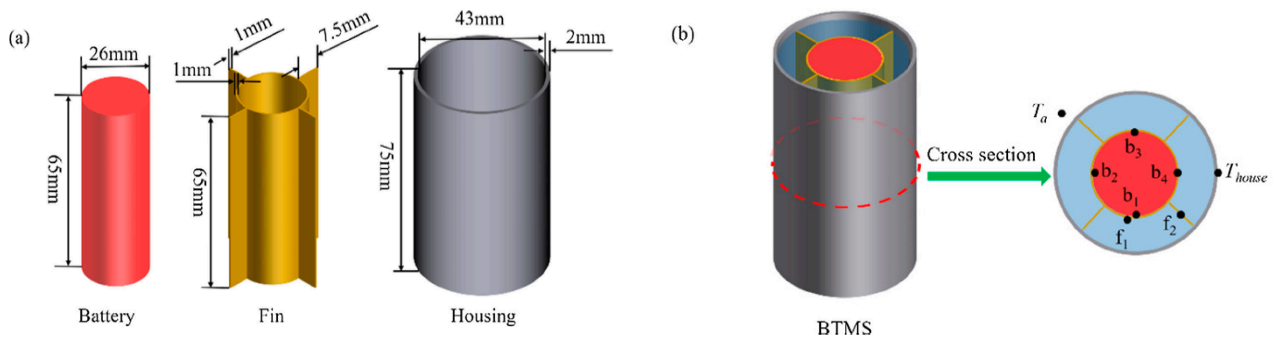


Figure 14. Schematic diagram of the PCM–fin-based BTMS: (a) configuration of BTMS and (b) locations of thermocouples [71].

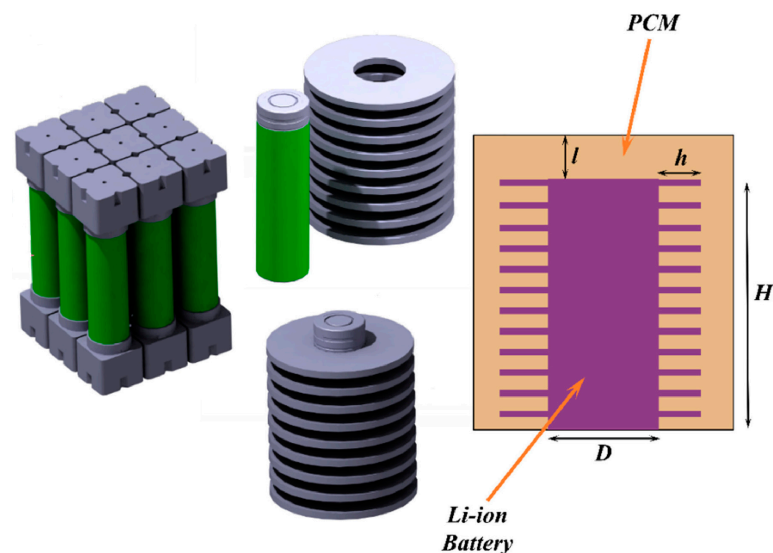


Figure 15. Schematic of the PCM–fin system geometry [72].

Numbers, locations, and shapes of fins can be arranged to reach the optimal thermal performance. Mansir et al. [73] investigated a cylindrical battery pack comprising three cylindrical cells enclosed in a space filled with PCMs. Their objective was to identify the optimal fin shape to maximize heat transfer. In another study, Qi et al. [74] conducted an optimization of the dimensions and spacing of fins installed on a LIB module. Through adjustments in fin height, fin width, and their respective distances, they investigated the resulting values of battery temperature and the quantity of liquid PCMs at various points during charging. The study demonstrated that an increase in fin size led to an augmentation of liquid PCMs during both the average charging period and the full charging time. The same effect was observed when increasing the distance between the fins. Notably, fin height had a more pronounced impact on both the quantity of liquid PCMs and battery temperature compared to alterations in fin width and spacing. Elevating fin height resulted in a reduction of both the maximum and average battery temperature throughout the charging process, including the full charging duration. Moreover, augmenting the distance between fins for fins of average size initially heightened the temperature and subsequently

reduced it. Meanwhile, an increase in fin width initially led to a reduction in temperature, followed by an increase.

Mechanical vibration plays a crucial role in the PCM-based BTMS, helping to restrict excessive temperature elevation and enhance the uniformity of temperature in lithium-ion batteries. Zhou et al. [75] examined the impact of mechanical vibration on a PCM-based module for thermal management in a single 26650 cylindrical cell, particularly under high ambient temperature and high discharge rate. Their findings indicated that mechanical vibration improved natural convection heat transfer, mitigating excessive temperature rise and promoting temperature uniformity. Notably, the most significant influence of mechanical vibration on the PCM-based BTMS occurred when the PCM thickness was 12 mm. Additionally, a vibration frequency of 10 Hz yielded the optimal cooling effect, resulting in a 28.05% lower temperature compared to scenarios without vibration. At a vibration frequency of 50 Hz, the temperature uniformity was maximized, achieving a maximum temperature difference of 3.86 K. When the vibration amplitude was 100 mm, the battery exhibited a maximum temperature difference of 1.89 K, corresponding to a 27.74% decrease in maximum temperature.

Enhancing the thermal conductivity of PCMs can be achieved through the addition of expanded graphite or by integrating them into metal foam. Idi et al. [76] developed and optimized a passive thermal management system by utilizing a composite of aluminum foam and paraffin RT27. The primary goal was to maintain the cell temperature below 27 °C during successive charge/discharge cycles. The findings demonstrated that the cell surface temperature was contingent on various factors, including the current rate, duration of charge and discharge cycles, and ambient temperature. The PCM was observed to effectively absorb the heat generated by the cell in a latent form during phase change. However, its limited thermal conductivity imposed constraints on its performance. The incorporation of aluminum foam enhanced the thermal management efficiency of the Li-ion cell. The optimization analysis demonstrated that underestimating the thickness, and consequently the mass of required PCM, resulted in exceedingly high temperatures. Furthermore, it was observed that increasing the volume of the PCM did not markedly influence the surface temperature of the cell.

Incorporating nanoparticles into phase-change materials (PCMs) represents an innovative strategy to enhance their thermal conductivity. Sazvar and Moqtaderi [77] performed a numerical analysis to explore cylindrical battery cooling systems utilizing PCMs. Their emphasis was on enhancing PCM's thermal conductivity through the incorporation of Cu nanoparticles, while also studying the latent heat and melting process of the nano-enhanced phase-change material (NEPCM). Their findings indicated that with increasing volume fractions, the rate of the melting process improved. The most significant enhancement, observed at a volume fraction of 10%, resulted in a 3.9% acceleration of the melting process. In another work, Talele and Zhao [69] investigated the comparative effect between organic paraffin wax PCMs and nano-enhanced PCMs to reduce NMC battery pack peak temperature. Their findings showed that the thermal effectiveness of the battery pack increased with nano-enhanced PCMs despite working at the harshest 2 C-rate and higher ambient temperature till 35 °C.

Some researchers endeavored to develop an analytical model and an exact solution to understand the phase-change process in such systems, aiming to identify the optimal operational conditions. Kermani et al. [78] introduced an innovative analytical model for the cooling process of cylindrical batteries utilizing PCMs. They examined two distinct types of PCMs and explored various scenarios involving different PCM properties and operational conditions. Additionally, they assessed the impact of considering the temperature field of the cells and the natural convection of the liquid PCM. Their findings revealed that PCM1, with a lower melting temperature and higher thermal conductivity compared to PCM2, required a thinner thickness, resulting in a more uniform temperature distribution across the pack. However, PCM2, with a significantly lower density, was preferable when the weight factor of the pack was crucial. In another study, Li et al. [79] introduced a

design optimization approach for BTMS incorporating PCMs. The optimization goal was to decrease the PCM mass while meeting two criteria: ensuring that the highest temperature difference in the BTMS remains below a specified limitation, and ensuring the necessary operational time to maintain the battery temperature within a secure range. To overcome the low thermal conductivity of conventional pure PCM, they utilized the EG/PA composite PCM.

BCM-cooled BTMS, while offering certain benefits, comes with its own set of disadvantages. One significant drawback is the limited heat transfer rate of PCMs compared to traditional cooling methods. The relatively low thermal conductivity of these materials can result in slower heat dissipation, potentially leading to temperature imbalances and hotspots within the battery pack. Moreover, the selection of appropriate PCMs involves careful consideration of factors such as melting point and compatibility, adding complexity to system design. The need to integrate PCM solutions into existing battery configurations may require modifications, contributing to increased costs and potential challenges in implementation. Additionally, PCM systems may not be as effective in high-temperature environments, limiting their applicability in certain conditions.

2.4. Hybrid BTMS

The hybrid method of thermal management for LIBs combines multiple cooling techniques to optimize performance. Typically, this approach integrates both active and passive cooling methods. Active cooling involves mechanisms such as liquid cooling or air cooling using fans or heat pumps, while passive cooling relies on natural heat dissipation through heat sinks or phase-change materials. By blending these methods, the hybrid approach aims to capitalize on the strengths of each, enhancing the overall efficiency of the thermal management system. This allows for better control over temperature regulation, particularly in high-demand situations or challenging environments. The hybrid method is often designed to provide a balance between the effectiveness of active cooling and the simplicity and reliability of passive solutions, ensuring optimal battery performance, longevity, and safety in diverse operating conditions. Table A4 (presented in Appendix A) summarizes the existing studies related to hybrid cylindrical BTMS. This table classified the previous studies based on the method, battery type, number of cells, load, cooling methods, and achievements.

2.4.1. Combining Air Cooling and Liquid Cooling

Air cooling and liquid cooling are two of the most common cooling methods for the thermal management of lithium-ion batteries. Considering that air cooling alone cannot be effective, it is combined with other systems. In fact, in this type of hybrid system, by adding air cooling to liquid cooling, the heating capacity of the system is increased. Air cooling is usually added to the system along with fins to help reduce the temperature and improve temperature uniformity in areas that are not in contact with liquid cooling. Angani et al. [80] introduced a battery thermal management system incorporating internal Zig-Zag plates. These plates were strategically placed around each cell, maximizing the surface area in contact with the Zig-Zag plates and thereby facilitating improved heat transfer. Two BTMS models were proposed: a bottom plate liquid-cooling system and a hybrid parallel pipe system for battery modules (Figure 16). In the battery module with a bottom plate liquid-cooling system, copper pipes were affixed to the bottom plate for coolant circulation. The heat generated by the cells underwent a three-step process: first, Zig-Zag plates extracted the heat from the cells; second, this heat was conducted to the support plates; and finally, it reached the bottom plate. As the coolant circulated through the pipe, the heat from the bottom plate was carried away. In the battery module with a hybrid parallel pipe cooling system, perforated Zig-Zag plates were employed to allow increased air circulation. Augmenting the airflow velocity reduced the cell temperature by dissipating more heat from the battery. The use of perforated Zig-Zag plates resulted in a reduced battery temperature due to enhanced heat transfer rates compared to non-

perforated Zig-Zag plates. A noteworthy increase in the convection heat transfer area ensured more cooling fluid comes into contact with the heat sink. After comparing the results, they demonstrated that the hybrid system achieved more uniform temperature, and a 28% improvement in thermal performance compared to the other system.

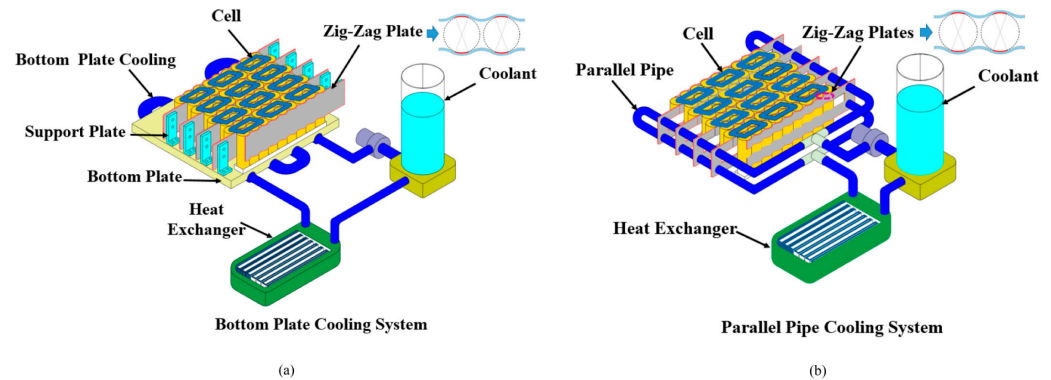


Figure 16. (a) Bottom plate liquid-cooling system. (b) Hybrid parallel pipe cooling system [80].

In another study, Zhou et al. [81] introduced a thermal management approach that integrated a half-helical coil and air jet impingement for cylindrical LIBs (Figure 17). This method involved transferring heat from the sides of the LIBs through a helical flow and dissipating it from the ends using air jet impingement. Their study revealed that the airflow and coolant flow configurations in the hybrid BTMS significantly impacted the system's heat dissipation. The adoption of a shortened fluid flow path jacket and positioning impinging air jets on both ends of the cylindrical structure resulted in minimizing the maximum temperature and temperature difference to 28.9 °C and 3.6 °C, respectively. Improved cooling performance was evident with an increase in the number of coil turns, attributed to the expanded heat transfer area. Alterations in airflow inlet velocity and inlet temperature had a minor effect on the temperature distribution of lithium-ion batteries. Decreased thermal contact resistance proved advantageous in enhancing the temperature consistency of the lithium-ion battery, with the temperature difference decreasing from 3.6 °C to 2.5 °C as contact resistance decreased from 0.0025 m²·K/W to 0.000625 m²·K/W.

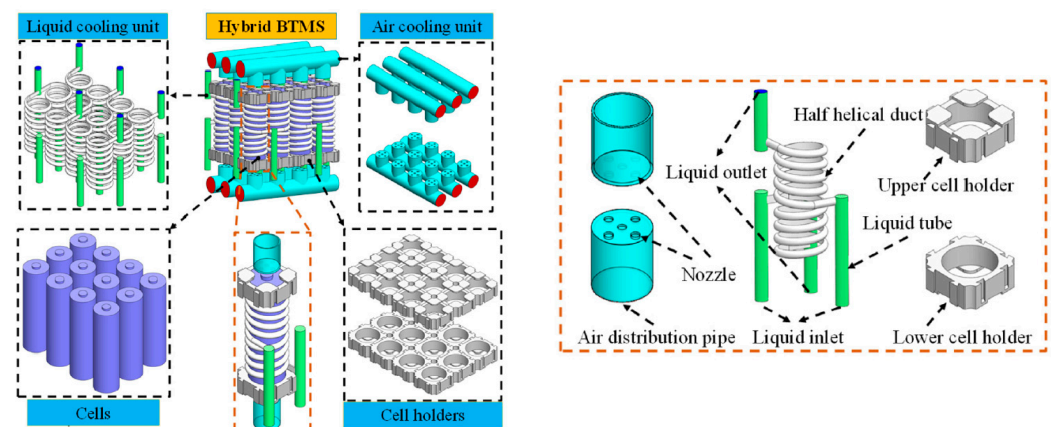


Figure 17. Schematic of a hybrid BTMS based on the half-helical coil coupled with air jet cooling [81].

One of the considerations of cylindrical modules is finding a way to increase the contact surface of the battery with the heat dissipation system. Xin et al. [82] presented a hybrid BTMS that combined air cooling and liquid cooling (Figure 18). Regularly spaced concave surfaces, matching the curvature of the battery's side surfaces, ensured close contact between the heat-conducting blocks (HCB) and the battery. Multiple HCBs were strategically positioned along the axial direction of the battery to promote uniform heat dissipation.

The cooling water circulating through the cooling channel progressively extracts heat from the aluminum block, absorbing it from the battery. In the liquid-cooled BTMS depicted in Figure 18, as the cooling water flows, it continuously absorbs the battery's heat, causing the water temperature to rise gradually and reducing the temperature difference between the battery and the water. Consequently, the heat dissipation of the battery diminishes in the direction of the cooling water flow, leading to a gradual increase in the corresponding battery temperature and the temperature difference among different batteries. Simultaneously, the cooling channel size affects the cooling performance of the battery module. The quantity, design, and arrangement of HCBs also influence the temperature uniformity of the battery and the heat exchange efficiency of the BTMS.

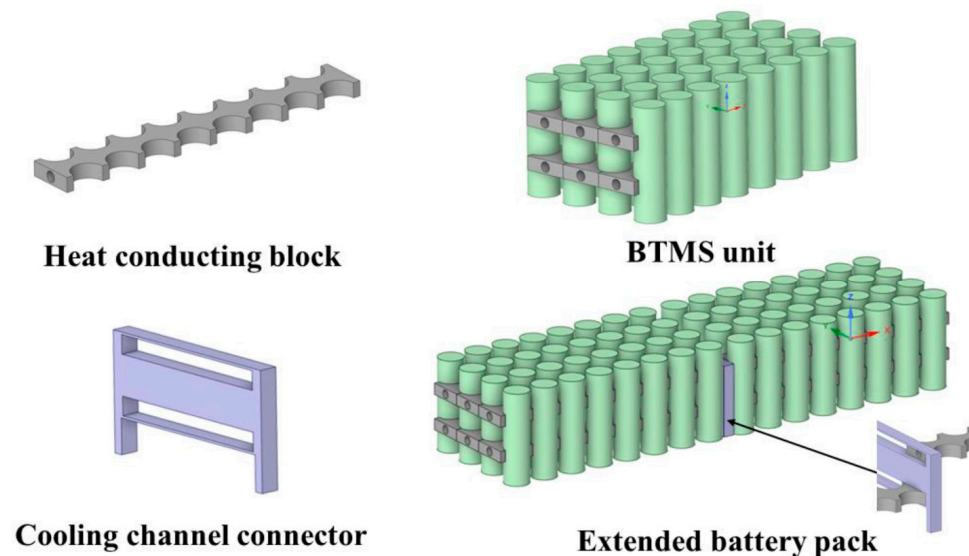


Figure 18. The schematic diagram of the BTMS 3D model [82].

2.4.2. Combining PCM Cooling and Liquid Cooling

The integration of phase-change materials and liquid cooling in a BTMS can combine the benefits of increased cooling capacity with reduced energy consumption. Yang et al. [83] introduced an innovative thermal management system for batteries, resembling a honeycomb structure, which incorporates a cooling plate with a hexagonal design incorporating bionic liquid mini-channels and PCMs. In Figure 19, the integration of the honeycomb-like battery thermal management system with the hexagonal cooling plate and PCMs is illustrated. A pump transports coolant from the water tank to the temperature control module, which subsequently circulates into the battery pack. Figure 19 details the battery module's structure, comprising cooling plates, cells, heat-conducting columns, and tubes. The hexagonal cooling plate incorporates bionic liquid mini-channels inspired by spider webs and honeycomb structures, with evenly distributed through-holes. Heat-conducting columns are positioned within the cell spaces, with their upper and bottom surfaces in contact with the cooling plate and their curved surfaces in contact with the cells. The surplus space in the heat-conducting columns is filled with the PCM. The coolant enters the battery module through the inlet, absorbs the generated heat, and returns to the water tank. In cases where the coolant's heat absorption rate is insufficient compared to the battery's heat generation rate, the PCM acts to absorb the excess heat.

Combining nanofluids with PCMs enhances battery performance during the charging process. Al-Rashed [84] utilized a combination of a hybrid nanofluid (NF) and nano-enhanced PCMs (Figure 20). The fluid within the battery, initially solid, acts as a PCM that undergoes melting due to the heat generated by the battery. Essentially, the battery provides the latent heat of vaporization for the PCM. During the material's solidification, the accumulated heat is transferred to the NF, with NF channels immersed in the PCM. Efficient performance requires careful consideration of the melting and freezing process

times. The NF flow within the channels removes heat from the PCM, leading to an increased temperature gradient. This enhancement in battery performance results from heightened velocity attributed to a reduction in the boundary layer thickness.

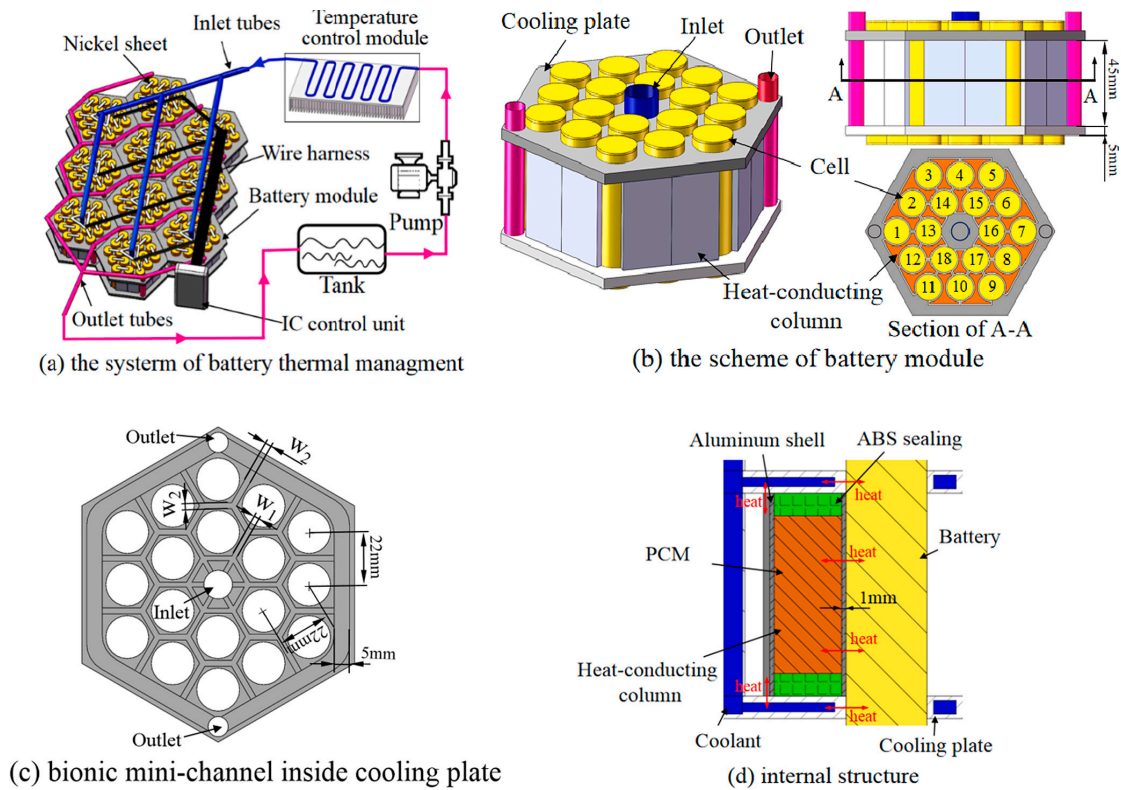


Figure 19. Scheme of the battery thermal management system [83].

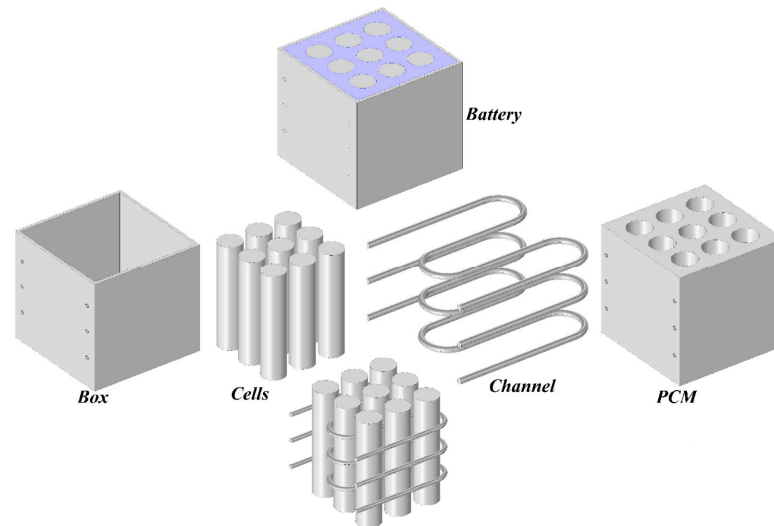


Figure 20. Schematic of a cooling system versus the proposed hybrid cooling system [84].

Combining PCMs and liquid cooling concurrently with a significant flow rate results in a decreased maximum temperature and a more uniform temperature distribution for the battery module, as opposed to employing either PCMs or liquid cooling in isolation. Xin et al. [85] devised a cooling system that incorporates both a composite phase-change material (graphite) and counterflow liquid cooling for a battery module consisting of 25 cylindrical batteries (Figure 21). They examined two distinct structures: the basic case and the composite case, exploring the effects of various parameters, such as thicknesses

of the composite phase-change material, fluid directions, mass fractions of expanded graphite, coolant velocities, and coolant temperatures, on the battery module's maximum temperature and temperature uniformity. Their findings revealed a notable reduction in the maximum temperature with a lower coolant inlet temperature, eventually reaching stability. However, this improvement in maximum temperature was accompanied by a decrease in temperature uniformity. In another study, Cao et al. [86] examined the effectiveness of a hybrid thermal management system utilizing water cooling and composite phase PCMs for cylindrical battery cells. The individual contributions of liquid cooling and PCMs were investigated independently. An et al. [87] introduced an innovative thermal management system employing a composite PCM consisting of paraffin (RT44HC) and expanded graphite (EG), coupled with liquid cooling. This system aimed to regulate the rise in temperature and difference of lithium-ion batteries within an optimal range, particularly at a discharge rate of 3 C.

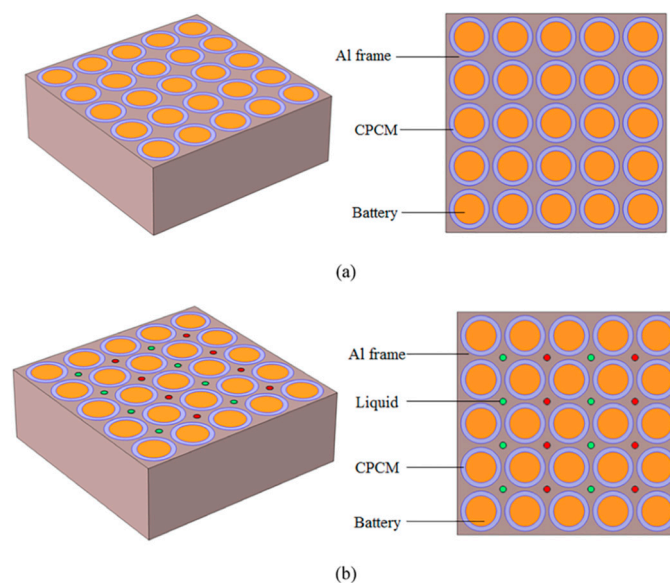


Figure 21. Structures of the battery module with (a) only CPCM and (b) the hybrid with liquid [85].

2.4.3. Combining Liquid Cooling and Heat Pipe

Liquid cooling results in additional energy consumption and creates temperature gradients within the battery pack. Despite numerous numerical and experimental proposals for cooling structures, working liquids, and strategies to address this issue, the challenge persists. The drawbacks of liquid cooling have spurred research efforts to integrate heat pipes with liquid cooling.

Heat pipes are components designed to dissipate heat efficiently by swiftly transferring thermal energy from one location to another. This process relies on the absorption of thermal energy (latent heat) when a liquid transforms into a gas and its subsequent release when the gas undergoes a phase change back into a liquid. Typically made of highly thermally conductive metals such as copper or aluminum, heat pipes consist of sealed metal pipes enclosing a small quantity of liquid known as a working fluid and a capillary structure (wick). Notably, this system operates without the need for external power or regular maintenance, incurs no operational costs, and demonstrates the capability to function over extended periods.

In order to present an efficient hybrid cooling method, Zheng et al. [88] introduced an innovative hybrid BTMS tailored for cylindrical batteries, incorporating micro heat pipe arrays (MHPA) and liquid cooling (Figure 22). The proposed system comprises Li-ion batteries (Type 18650), aluminum conduction elements, a U-shaped micro heat pipe array (MHPA), and cold plates. Positioned between two rows of batteries, the U-shaped MHPA efficiently draws heat from within the battery pack to the external environment. Liquid

channels on either side of the battery pack act as heat exchangers, facilitating the removal of heat as needed. Specially designed aluminum conduction elements are placed between the batteries and the MHPA to maximize surface contact, and thermal grease ensures effective system contact. The heat generated by the batteries is transferred to the MHPA through the aluminum conduction element, enhancing the heat transfer area. Subsequently, the MHPA transfers the heat to the cooling plate through the internal phase-change cycle, and the water in the cooling plate carries the heat away. The U-shaped configuration of the MHPA, resembling a flat heat pipe with independent microscale channels, enables efficient heat transfer. The evaporation section absorbs heat, initiating a phase-change cycle in the internal working fluid. This process transfers heat to the condensation section, ensuring high thermal conductivity and uniform temperature distribution. To optimize the heat exchange area with the cold plates, the MHPA is configured in a U shape.

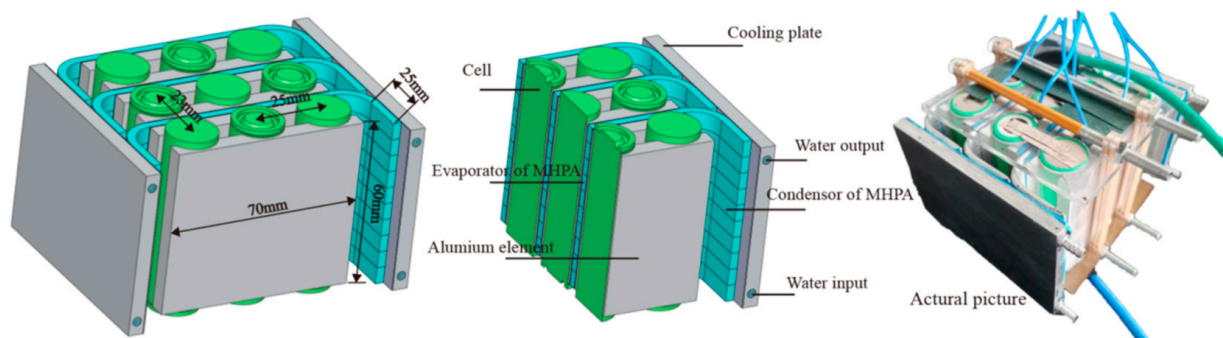


Figure 22. Geometry model of the designed hybrid battery module based on MHPA and liquid cooling [88].

2.4.4. Combining PCM Cooling and Heat Pipes

The thermal performance of a LIB pack can be strongly enhanced by the presence of PCMs and the heat pipe. The PCM exclusively absorbs or releases heat to the cell without participating in heat exchange with the environment, while the heat pipe is involved in exchanging heat with the surroundings. Incorporating a heat pipe alongside a PCM for heat removal can significantly enhance the system's thermal efficiency. When designing and manufacturing the hybrid cooling system, emphasis is placed on achieving lightweight and compact characteristics. The shape and structure of the cooling system are crafted to efficiently utilize the vacant space between tightly assembled cylindrical batteries, ensuring that the assembly process does not introduce additional volume to the battery module. Both the PCM tube and the heat pipe, including the fin structure, are constructed from aluminum, a material known for its lightweight properties and relatively low cost. Peng et al. [89] devised a cylindrical lithium-ion battery module featuring a compact hybrid cooling system integrating PCM and heat pipes. The batteries are closely arranged, and the vacant spaces between them are filled with either heat pipes or PCM tubes, as illustrated in Figure 23. The condensation section of the heat pipe is exposed to the surrounding environment. To ensure electric insulation, the battery module is enveloped in an epoxy board, and additional thermal insulation material is applied to minimize direct heat loss to the surroundings. The study revealed that, during the discharge process, the distribution of the PCM liquid fraction is non-uniform, with the outer layer and top section of the PCM melting first. Variations in heat dissipation rates among batteries, particularly under higher C-rate discharges, lead to temperature disparities among the batteries. Consequently, non-uniform PCM melting occurs, exacerbating the temperature differences between the batteries.

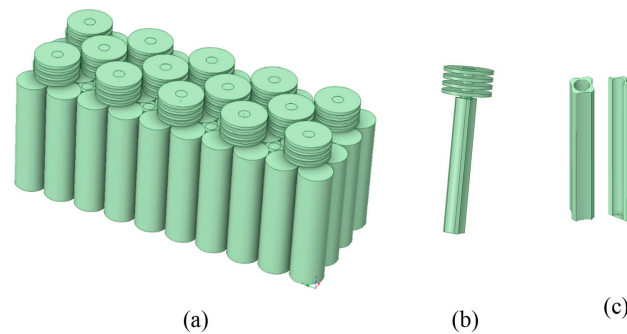


Figure 23. Configurations of (a) BTMS and battery module, (b) heat pipe, and (c) PCM tube [89].

3. Conclusions and Future Prospective

This paper presents a comprehensive review of the thermal management strategies employed in cylindrical lithium-ion battery packs. Lithium-ion batteries are sensitive to temperature fluctuations that can significantly impact their performance, safety, and lifespan. Maintaining an optimal temperature range is crucial to prevent overheating, which can lead to accelerated degradation, reduced capacity, and even safety hazards such as thermal runaway. Additionally, a well-designed thermal management system should also address temperature uniformity, ensuring that all cells within the battery pack experience consistent thermal conditions to avoid imbalances in performance and degradation. In addition, lightweight design is one critical parameter that should be considered.

In addition to all the criteria that should be considered for the thermal management systems of lithium-ion batteries, two important features specific to cylindrical batteries should also be considered. The thermal conductivity of cylindrical cells differs in different directions; therefore, the axial thermal conductivity is much more than the radial thermal conductivity. This feature makes the heat dissipation from the cell to the surrounding environment better through an axis form of heat transfer. The second issue is the geometry of cylindrical packs. Due to the geometry of the cylindrical cells, their placement in the modules comes with problems, such as the space between the cells, which makes it more difficult to remove heat and build a cooling system according to it. The cylindrical form factor imposes limitations on the design and integration of thermal management systems. Designing solutions that fit within the confined space while not compromising safety or performance remains a challenge.

The review covers four major thermal management techniques: air cooling, liquid cooling, PCMs, and hybrid methods. Air-cooling strategies are analyzed for their simplicity and cost-effectiveness, while liquid-cooling systems are explored for their superior heat dissipation capabilities. Phase-change materials, with their latent heat absorption and release properties, are evaluated as potential passive cooling solutions. Additionally, hybrid methods, combining two or more strategies, are discussed for their synergistic effects in achieving optimal thermal management. Figure 24 shows the comparison of different cooling methods of lithium-ion batteries.

Despite many studies, there are still challenges related to the thermal management of cylindrical lithium-ion batteries. Implementing advanced thermal management solutions can increase the overall cost of battery packs. Developing cost-effective strategies without compromising performance is an ongoing challenge. Future thermal management systems aim to enhance the overall performance and efficiency of cylindrical lithium-ion batteries. This includes optimizing heat dissipation to maintain safe operating temperatures, thus improving the battery's lifespan and performance. The utilization of advanced materials, such as novel thermal interface materials and PCMs, to enhance the thermal conductivity and heat dissipation capabilities of the battery systems should be encouraged. Additionally, the development of smart and adaptive thermal management systems that can dynamically respond to changing operating conditions, ensuring optimal thermal performance under varying loads and environmental conditions, merits future investigation. The need

to explore innovative cooling techniques to address specific challenges associated with cylindrical battery geometries can still be seen.

	Advantages	Disadvantages
Air cooling	<ul style="list-style-type: none"> • Low cost • Simple structure • High reliability • Easy maintenance 	<ul style="list-style-type: none"> • Low efficiency • Low cooling capacity • Noise (when using fan)
Liquid cooling	<ul style="list-style-type: none"> • Better efficiency • Higher cooling capacity • Flexibility in Design • Controllability • Reduced Noise (compared to air cooling) 	<ul style="list-style-type: none"> • Complex structure • Leakage problem • Need a large space • Heavyweight
PCM cooling	<ul style="list-style-type: none"> • Low cost • Providing temperature uniformity • High efficiency • Simple Structure 	<ul style="list-style-type: none"> • Leakage problem • Low thermal conductivity • Heavyweight • Flammability

Figure 24. Comparison between cooling strategies.

Due to the limited thermal conductivity of air-cooling systems, their widespread adoption is restricted. Therefore, there is a need for a high thermal management system that combines multiple traditional cooling methods. Researchers should prioritize the integration of liquid cooling, PCM cooling, and heat pipes. Hybrid systems, specifically combining liquid cooling and PCM cooling, are recommended due to the higher thermal conductivity of liquids and the greater latent heat of PCMs. While a PCM's standalone thermal conductivity may not be optimal, it can be improved by incorporating a conductive compound. Researchers should explore conductive materials and nanoparticles that enhance PCM conductivity when added. Significantly increasing the thermal conductivity of a PCM could make it the most efficient cooling system when combined with other cooling methods. Although heat pipe cooling is effective, its limited contact area poses a major challenge. To address this, the use of a conductive cold plate is recommended to increase the contact area of both conventional and pulsating heat pipes.

An important future study is the scale-up of thermal management systems. The critical question to raise is: what changes are to be made for battery packs of different sizes including the same type of cells? Take liquid channel cooling for example: to ensure a cell in a pack operates in the same temperature ranges, the amount of heat that has to be carried away by the coolant should be the same. However, as the coolant temperature increases faster in a larger pack, the temperature difference between the cell and local coolant reduces faster; as such, the coolant flow rate has to be increased to ensure a similar operation temperature. However, beyond a certain limit, increasing the coolant flow rate does not actually change the thermal performance; instead, it increases the pumping power. At this point, it might be helpful to increase the number of cooling channels, although geometrical and weight limitations should be considered. Overall, there is no straightforward scale-up strategy for a thermal management system. Parameters such as flow rate, cooling channel number, and others need to be adjusted simultaneously, which further depend on the quantitative prediction and optimization of a BTMS.

Author Contributions: Conceptualization, M.A.-E. and P.Z.; investigation, M.A.-E.; resources, M.A.-E. and P.Z.; data curation, M.A.-E.; writing—original draft preparation, M.A.-E.; writing—review and editing, M.A.-E. and P.Z.; supervision, P.Z.; project administration, P.Z.; funding acquisition, P.Z. All authors have read and agreed to the published version of the manuscript.

Funding: The research was funded by start-up funding at the University of Tennessee Space Institute.

Data Availability Statement: Not applicable.

Acknowledgments: Thanks to the invitation from the special issue editors, with the waiver for open access publication.

Conflicts of Interest: The authors declare no conflicts of interest.

Appendix A

Table A1. Summary of research on air-cooling BTMS (N.M: not mentioned).

Reference	Method	Type	Number	Load	Arrangement	Flow Regime	Airflow	T _{max} (K)	ΔT (K)	Main Focus	Other Objectives
Yang et al. [10]	Exp-Num	18650	37	3	Hexagonal	Turbulent	8–12 m/s	311	1.7	Air distribution plate	Structure parameters
Zhou et al. [36]	Exp-Num	18650	9	3–5	Aligned	Laminar	48 L/min	305.7	3	Air distribution pipe	Inlet pressure, discharge rate
Yang et al. [35]	Exp-Num	18650	1	3	-	Laminar	0.1–1.5 m/s	308	5	Optimization, bionic surface structure	Structure parameter, inlet velocity
Zhou et al. [90]	Exp-Num	18650	1	5	-	Laminar	0.1–1 m/s	310.191	1.978	Optimization, honeycomb cooling structure	Structure parameter
Hasan et al. [91]	Num	18650	52	N.M	Staggered	Turbulent	Re = 1.5–3 × 10 ⁴	324	3.5	Turbulence intensity	Reynolds number
Zhao et al. [92]	Num	18650, 26650, 42110	24	5	Aligned	Turbulent	0.1–10 m/s	307	4		Gap spacing, environment temperatures
Li et al. [93]	Exp-Num	N.M	32	N.M	Aligned	Laminar	0.02–20 m/s	310	3.5		
Kummitha et al. [38]	Num	32700	9	5	Aligned	Turbulent	N.M	301.5	0.26	Cell holders' jacket fins	
Hai et al. [94]	Num	N.M	50	N.M	Aligned		Re = 400	301	0.93		Structure parameter
Mahamud et al. [43]	Num	N.M	8	1–10	Aligned	Turbulent	1 m/s	303	4	Reciprocating flow	Reciprocation period, cell spacing, coolant flow rate
Lu et al. [39]	Num	18650	14	0.5	Stagger-arranged	Laminar	10 ⁻⁴ kg/s	303.6	10.5		Channel size, inlet and outlet locations, channel length
Ji et al. [40]	Exp-Num	18650	16	0.6–2	Aligned	Laminar	0.001 m/s	307	2.7	Optimization	Structure parameters
Wang et al. [44]	Num	18650	24	1.5	Aligned	Turbulent	2–5 m/s	304.5	0.97	Optimization	Structure parameters

Table A1. Cont.

Reference	Method	Type	Number	Load	Arrangement	Flow Regime	Airflow	T _{max} (K)	ΔT (K)	Main Focus	Other Objectives
Li et al. [95]	Exp-Num	21700	1	0.5	-	N.M		300		Optimization	
Saechan et al. [96]	Num	18650	40	0.5–2	Aligned	Turbulent	1 m/s	315	5.2		Structure parameters
Ruhani et al. [97]	Num	18650	9	1	Aligned	Laminar	Re = 80–140				Reyolds number
Kausthubharam et al. [41]	Num	18650	36	1.4	Aligned	Laminar	0.1–1 m/s	304.2	0.4	Thermal interface material	Structural and operational parameters on
Xun et al. [98]	Num	18650	20	2	Aligned	Laminar	N.M	319	5		Number of cooling channels, channel size
Zhao et al. [99]	Num	18650	71	5	Stagger-arranged	Laminar	0.1 m/s	310	0.7	Multiple short channels	Structural and operational parameters on
Yang et al. [100]	Exp-Num	18650	8	1–4	Aligned	Turbulent	0.87–1.03 m/s	305	2.1		Structure parameters
Fan et al. [101]	Num	18650	32	0.6–4	Aligned, staggered, and cross	Laminar—Turbulent	0.1–10 m/s	305	1.4		Discharge rate, inlet temperature, energy efficiency
Cen et al. [102]	Exp-Num	18650	1	0.5–1.5	-	N.M	N.M	305	1.5		
E et al. [103]	Exp-Num	18650	60	0.5–1	Aligned	Laminar	2 m/s	307.2	2.4		Structure parameters
Chen et al. [104]	Num	18650	50			Laminar		309.2			
Hai et al. [105]	Num	18650	16	N.M	Aligned	Laminar	0.08–0.15 m/s	307.8	N.M		Structure parameters
Wang et al. [106]	Num	18650	25	1–3	Aligned		1 m/s	303	N.M		
Shahid et al. [107]	Exp-Num	18650	32	2	Aligned	Turbulent	N.M	301	1.1		Structure parameters
Zhang et al. [108]	Num	18650	25	3	Aligned	Turbulent	2.89×10^{-3} kg/s	308.8	1.493		Structure parameters
Hasan et al. [109]	Num	N.M	30	N.M	Aligned	Turbulent	Re = 15,000–30,000	303	N.M	Optimization	

Table A1. Cont.

Reference	Method	Type	Number	Load	Arrangement	Flow Regime	Airflow	T _{max} (K)	ΔT (K)	Main Focus	Other Objectives
Yang et al. [110]	Num	N.M	6	N.M	Aligned—staggered	Turbulent	0.01326 m ³ /s	304.4	N.M	Optimization	Structure parameters
Shahid et al. [111]	Exp-Num	18650	32		Aligned	Turbulent	2–32 m/s	301.2	4.09	Vortex generators	
Peng et al. [112]	Exp-Num	18560	20	2	Aligned	Laminar	1 m/s	301.8	N.M		
Hai et al. [113]	Num	18650	16	N.M	Aligned—non-aligned	N.M	0.03–0.09 m/s	311	N.M		
Marambio et al. [114]	Num-Exp	N.M	25–30	1	Aligned	N.M	2, 2.5 m/s	309	N.M	Predicting the surface temperature	
Qin et al. [115]	Num-Exp	18650	4	1–4	Aligned	Laminar		321.2	4.5	Internal finned structure	
Shahid et al. [111]	Num-Exp	18650	32	2	Aligned		6 m/s	301.2	4.1		
Saw et al. [116]	Num	38120	24	3	Aligned		30 g/s	308.8	4		
Yu et al. [117]	Num-Exp	18650	66	0.5	Staggered		0.8 m/s	309.1	2.8		
Wang et al. [118]	Num-Exp	N.M	30	1	Aligned		8 m/s	55	17.6		
Wang et al. [37]	Num-Exp	N.M	24	1	Aligned		1 m/s	306.7	2.9		

Table A2. Summary of research on liquid-cooling BTMS (N.M: not mentioned).

Reference	Method	Type	Number	Load	Coolant	Inlet Flow	T _{max} (K)	ΔT (K)	Main Focus	Other Objective
Lai et al. [58]	Num	18650	1	5	Water	10 ⁻⁴ kg/s	313	4.3137	Weight, thermal conductive structure (TCS)	Mass flow rate, inner diameter, contact surface height, contact surface angle
Gao et al. [48]	Exp-Num	18650	16	2	Water	360 mL/min	310.03	1.96	Gradient channel	Flow direction, number of channel segments, segment lengths, inlet flow rate
Yates et al. [49]	Num	18650	4	5	Water	5 × 10 ⁻⁵ kg/s	313	3.15	Geometric modification	Channel number, hole diameter, mass flow rate, inlet locations
Li et al. [50]	Num	18650	20	1–4	Water	10 ⁻³ kg/s	303.26	1.984	Geometric modification	Inlet velocity, flow direction, channel cross-section shapes, battery spacing, pressure drop
Xia et al. [51]	Num	N.M	1	Not mentioned	Water	Not mentioned	322.95	2.38	Fractal tree-like channels	Pressure drop
Wang et al. [52]	Exp-Num	18650	20	3	Water	80 mL/min	308.89	4.17	Cooling mode (serial cooling and parallel cooling)	Flow rate, flow direction
Kim et al. [53]	Exp-Num	18650	36	2–10	Water	0.016 kg/s	323.15	N.M	Two different types of cold plates	
Xie et al. [67]	Num	18650	48	2	Water	0.2 m/s	304.01	4.99	Adding baffles	Number, height, and position of baffles
Sun et al. [119]	Num	21700	1	4	Water and ethylene glycol	7.95 × 10 ⁻²	306.44	1.0605	Different channel structures	Channel diameter, inlet velocity
Sheng et al. [54]	Exp-Num	21700	7	1–2	Water	10 ⁻⁴ L/s	309.73	1.05	Cellular liquid cooling jacket	Flow rate, channel dimension
Chang et al. [120]	Exp-Num	18650	2	0.5	Water and ethylene glycol	0.65 L/min	308.15	1.67	Reciprocating liquid flow	Flow rate, ambient temperature
Xu et al. [55]	Num	18650	32	1–3	Water	0.1 m/s	30.3.2	3.69	Wrench-shaped	Bifurcation position, pressure drop

Table A2. Cont.

Reference	Method	Type	Number	Load	Coolant	Inlet Flow	T _{max} (K)	ΔT (K)	Main Focus	Other Objective
Sarchami et al. [63]	Exp-Num	18650	6	5	Alumina nanofluid	10–120 mL/min	305.13	2.01	Copper sheath	C-rate, alumina nanoparticle concentration, inflow velocity, stair channel geometry
Dong et al. [121]	Num	18650	1	5	Water	1.94×10^{-3} kg/s	305.51	6.98	Double helix structure	Mass flow rate, helix groove pitch, flow diameter
Zhao et al. [99]	Num	18650	71	5	50% water + 50% methanol	0.1 m/s	309.9	2.2	Geometric modification	
Xiong et al. [60]	Num	26650	1	0.5–2	Water	0.4 g/s	302.972	3.858	Bionic flow channel structure	Channel height, channel length, mass flow rate
Shan et al. [59]	Num	18650	10–30	2	Water	0.02 m/s	300.47	2.09	Lightweight design	Diameter of the coolant channel, contact surface angle, flow direction layout
Liang et al. [61]	Num	18650	5	3	Water	6×10^{-7} m ³ /s	313.116	4.339	Lightweight design, lower power consumption	Flow rate, inlet water temperature, number of components
Tete et al. [57]	Num	18650	25	0.5–5	Water	0.01 m/s	301.15	0.12	Cell casings	Discharge rate
Tousi et al. [62]	Num	18650 21700	12	1–2	DI-water and AgO nanofluid	0.2–0.28 m/s	306.65	0.67	Using nanofluid	Pressure drop, flow rate, nanoparticle volume fraction, discharge C-rate
Li et al. [122]	Num	18650	40	3	Water	0.03–0.3 m/s	302.4	2.88	Comparing serpentine channel and the U-shaped channel, optimization	Pressure drop
Wang et al. [66]	Num	18650	90	5	Water	0.2–0.5 m/s	302.15	3.3	Optimization	Inlet velocity, channel number, contact angle
Liu et al. [123]	Num	18650	24	3, 5	Water and liquid metal	0.5 m/s	311.85	3.3	Liquid metal	Pumping power, flow velocity, structure

Table A2. Cont.

Reference	Method	Type	Number	Load	Coolant	Inlet Flow	T _{max} (K)	ΔT (K)	Main Focus	Other Objective
Yao et al. [124]	Exp-Num	18650	18	3	Water	N.M	311.75	1.9	Bionic spider web channel	Discharge rates, fluid flow arrangements, Reynolds number
Zeng et al. [64]	Exp-Num	18650	32	1–6	Water	0.5 m/s	303.83	0.739	Reciprocating flow	Velocity, reciprocating period
Zhao et al. [125]	Num	18650	71	0.5–5	Water	0.5 m/s	308.15	1		C-rate, flow rate, interfacial area
Esmaili et al. [126]	Num	18650	16	2	Water	0.00399 kg/s	301.4	0.78	Twisted tapes	Twist pitches, twisted tape edges, intensified ratios
Zhou et al. [127]	Num	18650	9	5	Water	3×10^{-4} kg/s	303.65	4.6	Half-helical duct	Mass flow rate, pitch and number of ducts, flow direction, duct diameter
Rao et al. [128]	Num	18650	24	3	Water	0.05–0.3 m/s	302.6	2.7	Contact surface	Block length, inlet velocity
Zhao et al. [129]	Num	42110	1	N.M	Water	10^{-3} kg/s	300	1.2	Geometric modification	Mini-channel quantity, flow rate, flow direction
Huang et al. [130]	Exp-Num	18650	48	1–5	Water	$1-8 \times 10^{-3}$ kg/s	304		Hysteresis time	Discharge rate, flow rate, heat transfer coefficient
Hasan et al. [131]	Num	18650	52	N.M	SiO ₂ -water, Al ₂ O ₃ water, ZnO water, CuO water Nanofluid		313		Using nanofluid	Different Reynolds number, pumping power
Bohacek et al. [132]	Exp-Num	18650	96	1	Water	0.1–0.7 L/min	308	4.6	Optimization	Flow rate
Ma et al. [65]	Num		2	1	Water	0.1–1 m/s	305	2	Optimization	
Lv et al. [133]	Exp-Num	21700	25	1–3	Water	0.44 m/s	310.8	4	Spacing	
Liu et al. [56]	Num	26650	25	1.3	Water	0.025–0.4 m/s	308.1	2.25	Geometric modification	Flow velocity, tube diameter
An et al. [134]	Exp	18650	8	1.4	Water	0.05–0.35	308.15	0.7	Increasing contact surface	High-temperature environment, SOC of the battery module

Table A3. Summary of research on PCM-cooling BTMS.

Reference	Method	Type	Number	Load	PCM Composite	Melting Point (K)	Thermal Conductivity (W/(m·K))	T _{max} (K)	ΔT (K)	Main Focus
Idi et al. [76]	Exp-Num	18650	1	1–4.5	Paraffin aluminum foam	300.15–331.15	0.15–0.2	300	1.5	
Lamrani et al. [135]	Num	21700	24	3	RT-31, RT-35 HC, A-32H	300–309	0.2–0.22	305	3	
Kermani et al. [78]	Num	18650	15	2–10	Chloride hexahydrate (CaCl ₂ ·6H ₂ O) and paraffin wax	302–309	0.18–1.008	303	2	Optimization, thermophysical properties of the PCM, rate of charge/discharge
Zhou et al. [75]	Num	18650	1	2	<i>n</i> -octadecane	301.15	0.152	332.36	1.89	Mechanical vibration frequency, vibration amplitude
Karimi et al. [136]	Exp	18650	1		Paraffin mixture	312–318	0.22	309	3	Nanoparticles
Lv et al. [137]	Exp	18650	24	1, 2.5, 3.5	Paraffin, expandable graphite, low-density polyethylene	317–323	0.16–0.38	321	3.9	
Khaboshan et al. [70]	Num	18650	1	3	<i>n</i> -eicosane PCM and metal foam	309.55	0.423	310.6		Fin shapes
Chen et al. [72]	Num	18650	1	0.5–1.7	Paraffin with alkane chain		0.358	315		Number of fins
Bias et al. [138]	Exp-Num	18650	1	3	Paraffin with alkane			314.9	1.5	
Mansir et al. [73]	Num	18650	3	2.4	Paraffin		0.358			Fin arrangement
Liu et al. [139]	Num	18650	1	1–3	Paraffin wax	311.15	0.2	314	1.48	Ambient temperature, fin shape
Qi et al. [74]	Num	18650	1	1–4	Paraffin wax			325		Optimization, fin structure
Li et al. [79]	Num	18650	4		Expanded graphite (eg)/paraffin (pa)	317			2.9	Optimization, mass of PCM
Wang et al. [140]	Num	18650	21			302		311		
Sun et al. [71]	Num	18650	1		Paraffin wax	313–317	0.2			Fin structure

Table A4. Summary of research on hybrid BTMS.

Reference	Method	Type	Number	Load	Cooling Method		Flow Regime	T _{max} (K)	ΔT (K)	Main Focus
Yang et al. [83]	Exp-Num	18650	18	2–4	Liquid cooling	PCM	Laminar	312	3.5	Structure parameters, working parameters, and conditions
Zhou et al. [81]	Exp-Num	18650	1	4	Liquid cooling	Air cooling	Turbulent	303	2	Different schemes, inlet velocity, contact resistance
Xin et al. [82]	Exp-Num	18650	32	3	Liquid cooling	Air cooling	Laminar	303.9	0.58	Heat-conducting blocks, mass flow rate
Angani et al. [80]	Exp-Num	21700	54	1, 1.25	Liquid cooling	Air cooling	Laminar	305	1.4	Structure parameters, airflow
Wang et al. [141]	Num	18650	48		Liquid cooling	Gas cooling	Turbulent	316.5		Airflow, turbulence intensity
Chen et al. [142]	Exp-Num	18650	24	4	Liquid cooling	PCM	Laminar	319.7	2.9	Mass flow rate
Behi et al. [143]	Exp-Num	18650	24	1.5	Heat pipe	Air cooling	Laminar	310.2		
Kong et al. [144]	Exp-Num	21700	6	3	Liquid cooling	PCM	Laminar	307		Cell-to-cell spacing, channel number, coolant velocity
Jiang et al. [145]	Num		9		Liquid cooling	PCM		308		
Khan et al. [146]	Num	18650	1	3	Air cooling	PCM	Laminar	303		Heat transfer coefficient, melting PCM content
Jilte et al. [147]	Num	18650	1	5	Liquid cooling	PCM		307.53		Nanoparticle concentration, structure parameters, melting behavior
Almehmadi et al. [148]	Num	18650	1		Air cooling	PCM	Laminar	304		Flow rate, PCM location
Zeng et al. [88]	Exp-Num	18650	9	1.3	Liquid cooling	Heat pipe		314.18	2.16	Optimization, design parameters
Mashayekhi et al. [149]	Exp-Num	18650	1	1–4	Liquid cooling	PCM		308	0.9	Nanofluid, power consumption, flow rate
Tian et al. [150]	Num	18650	9		Air cooling	PCM		303		Cost of electricity consumption
Gholami Zadeh et al. [151]	Num	18650	12	5	Liquid cooling	PCM		318.1	3.60	Aging analysis
Shahid et al. [152]	Exp-Num	18650	9	1–7	Liquid cooling	PCM	Laminar	302.5	1.8	
Wang et al. [153]	Exp	18650	40	2	Heat pipe	PCM		320.8	2.5	
Zhao et al. [154]	Exp	18650	12	5	Heat pipe	PCM		320	5	
Weng et al. [155]	Exp-Num	18650	1	1–4	Air cooling	PCM		303.6	1.6	
Faizan et al. [156]	Exp-Num	18650	1	0.2–2	Liquid cooling	PCM	Laminar	307	1.6	

Table A4. Cont.

Reference	Method	Type	Number	Load	Cooling Method		Flow Regime	T _{max} (K)	ΔT (K)	Main Focus
Cao et al. [86]	Exp-Num	18650	20	3	Liquid cooling	PCM	Laminar	315	1.2	Mass fraction of PCMs
Chavan et al. [157]	Exp-Num	18650	4	1	Liquid cooling	Heat pipe		311.4		
An et al. [87]	Num	18650	25	3	Air cooling	PCM	Laminar	319.4	2	Mass fraction of PCM, channel layout
Peng et al. [89]	Num	18650	4	0.5–2	Heat pipe	PCM		308	1	PCM properties
Zhao et al. [158]	Exp-Num	18650	40	0.96–1.92	Air cooling	PCM	Turbulent	312.53	4.70	Optimization, PCM properties
Li et al. [159]	Exp-Num	18650	40	2–4	Liquid cooling	Air cooling	Turbulent	314	2	Optimization, flow direction
Bamdezh et al. [160]	Num	18650	1	3	Liquid cooling	PCM	Laminar	304	2.7	
Jiang et al. [161]	Num	18650	9	1	Liquid cooling	PCM	Laminar	322		Nanoparticles
Qi et al. [162]	Num	18650	9		Air cooling	PCM	Laminar	305		
Lee et al. [163]	Num	18650	1		Air cooling	PCM		303		
Akkurt et al. [164]	Num	21700	3	3–4	Air cooling	PCM	Laminar	304		
Xin et al. [85]	Num	18650	25	5	Liquid cooling	PCM	Laminar	318.4	3.49	PCM properties
Al-Rashed [84]	Num		9		Liquid cooling	PCM	Laminar	312		Optimization
Cao et al. [165]	Num	18650	40	1–4	Liquid cooling	PCM	Laminar	313	5	Delayed cooling
Junwei et al. [166]	Exp	18650	15	1–6	Liquid cooling	PCM		310.28	3.75	

References

1. Ahmed, A.A.; Nazzal, M.A.; Darras, B.M.; Deiab, I.M. Global Warming Potential, Water Footprint, and Energy Demand of Shared Autonomous Electric Vehicles Incorporating Circular Economy Practices. *Sustain. Prod. Consum.* **2023**, *36*, 449–462. [\[CrossRef\]](#)
2. Halkos, G.E.; Gkampoura, E.C. Reviewing Usage, Potentials, and Limitations of Renewable Energy Sources. *Energies* **2020**, *13*, 2906. [\[CrossRef\]](#)
3. Behabtu, H.A.; Messagie, M.; Coosemans, T.; Berecibar, M.; Fante, K.A.; Kebede, A.A.; Van Mierlo, J. A Review of Energy Storage Technologies' Application Potentials in Renewable Energy Sources Grid Integration. *Sustainability* **2020**, *12*, 10511. [\[CrossRef\]](#)
4. Kebede, A.A.; Kalogiannis, T.; Van Mierlo, J.; Berecibar, M. A Comprehensive Review of Stationary Energy Storage Devices for Large Scale Renewable Energy Sources Grid Integration. *Renew. Sustain. Energy Rev.* **2022**, *159*, 112213. [\[CrossRef\]](#)
5. Chombo, P.V.; Laoonual, Y. A Review of Safety Strategies of a Li-Ion Battery. *J. Power Sources* **2020**, *478*, 228649. [\[CrossRef\]](#)
6. Simon, P.; Gogotsi, Y. Perspectives for Electrochemical Capacitors and Related Devices. *Nat. Mater.* **2020**, *19*, 1151–1163. [\[CrossRef\]](#)
7. Yang, L.; Nik-Ghazali, N.N.; Ali, M.A.H.; Chong, W.T.; Yang, Z.; Liu, H. A Review on Thermal Management in Proton Exchange Membrane Fuel Cells: Temperature Distribution and Control. *Renew. Sustain. Energy Rev.* **2023**, *187*, 113737. [\[CrossRef\]](#)
8. Sun, X.; Zhang, Y.; Zhang, Y.; Wang, L.; Wang, K. Summary of Health-State Estimation of Lithium-Ion Batteries Based on Electrochemical Impedance Spectroscopy. *Energies* **2023**, *16*, 5682. [\[CrossRef\]](#)
9. Zhang, X.; Li, Z.; Luo, L.; Fan, Y.; Du, Z. A Review on Thermal Management of Lithium-Ion Batteries for Electric Vehicles. *Energy* **2022**, *238*, 121652. [\[CrossRef\]](#)
10. Yang, W.; Zhou, F.; Chen, X.; Li, K.; Shen, J. Thermal Performance of Honeycomb-Type Cylindrical Lithium-Ion Battery Pack with Air Distribution Plate and Bionic Heat Sinks. *Appl. Therm. Eng.* **2023**, *218*, 119299. [\[CrossRef\]](#)
11. Mousavi, S.; Zadehkabir, A.; Siavashi, M.; Yang, X. An Improved Hybrid Thermal Management System for Prismatic Li-Ion Batteries Integrated with Mini-Channel and Phase Change Materials. *Appl. Energy* **2023**, *334*, 120643. [\[CrossRef\]](#)
12. Ham, S.H.; Jang, D.S.; Lee, M.; Jang, Y.; Kim, Y. Effective Thermal Management of Pouch-Type Lithium-Ion Batteries Using Tab-Cooling Method Involving Highly Conductive Ceramics. *Appl. Therm. Eng.* **2023**, *220*, 119790. [\[CrossRef\]](#)
13. Liu, C.; Shen, W.; Liu, X.; Chen, Y.; Ding, C.; Huang, Q. Research on Thermal Runaway Process of 18650 Cylindrical Lithium-Ion Batteries with Different Cathodes Using Cone Calorimetry. *J. Energy Storage* **2023**, *64*, 107175. [\[CrossRef\]](#)
14. Kim, E.; Song, J.; Dzakpasu, C.B.; Kim, D.; Lim, J.; Kim, D.; Park, S.; Lee, H.; Kwon, T.S.; Lee, Y.M. Degradation Behavior of 21700 Cylindrical Lithium-Ion Battery Cells during Overdischarge Cycling at Low Temperatures. *J. Energy Storage* **2023**, *72*, 108627. [\[CrossRef\]](#)
15. Sharma, D.K.; Prabhakar, A. A Review on Air Cooled and Air Centric Hybrid Thermal Management Techniques for Li-Ion Battery Packs in Electric Vehicles. *J. Energy Storage* **2021**, *41*, 102885. [\[CrossRef\]](#)
16. Talele, V.; Patil, M.S.; Panchal, S.; Fraser, R.; Fowler, M. Battery Thermal Runaway Propagation Time Delay Strategy Using Phase Change Material Integrated with Pyro Block Lining: Dual Functionality Battery Thermal Design. *J. Energy Storage* **2023**, *65*, 107253. [\[CrossRef\]](#)
17. Liu, X.; Ai, W.; Naylor Marlow, M.; Patel, Y.; Wu, B. The Effect of Cell-to-Cell Variations and Thermal Gradients on the Performance and Degradation of Lithium-Ion Battery Packs. *Appl. Energy* **2019**, *248*, 489–499. [\[CrossRef\]](#)
18. Troxler, Y.; Wu, B.; Marinescu, M.; Yufit, V.; Patel, Y.; Marquis, A.J.; Brandon, N.P.; Offer, G.J. The Effect of Thermal Gradients on the Performance of Lithium-Ion Batteries. *J. Power Sources* **2014**, *247*, 1018–1025. [\[CrossRef\]](#)
19. Song, Z.; Yang, N.; Lin, X.; Pinto Delgado, F.; Hofmann, H.; Sun, J. Progression of Cell-to-Cell Variation within Battery Modules under Different Cooling Structures. *Appl. Energy* **2022**, *312*, 118836. [\[CrossRef\]](#)
20. Raijmakers, L.H.J.; Danilov, D.L.; Eichel, R.A.; Notten, P.H.L. A Review on Various Temperature-Indication Methods for Li-Ion Batteries. *Appl. Energy* **2019**, *240*, 918–945. [\[CrossRef\]](#)
21. Jinasena, A.; Spitthoff, L.; Wahl, M.S.; Lamb, J.J.; Shearing, P.R.; Strømman, A.H.; Burheim, O.S. Online Internal Temperature Sensors in Lithium-Ion Batteries: State-of-the-Art and Future Trends. *Front. Chem. Eng.* **2022**, *4*, 804704. [\[CrossRef\]](#)
22. Zheng, Y.; Che, Y.; Hu, X.; Sui, X.; Stroe, D.I.; Teodorescu, R. Thermal State Monitoring of Lithium-Ion Batteries: Progress, Challenges, and Opportunities. *Prog. Energy Combust. Sci.* **2024**, *100*, 101120. [\[CrossRef\]](#)
23. Zhang, J.; Wu, B.; Li, Z.; Huang, J. Simultaneous Estimation of Thermal Parameters for Large-Format Laminated Lithium-Ion Batteries. *J. Power Sources* **2014**, *259*, 106–116. [\[CrossRef\]](#)
24. Drake, S.J.; Wetz, D.A.; Ostanek, J.K.; Miller, S.P.; Heinzl, J.M.; Jain, A. Measurement of Anisotropic Thermophysical Properties of Cylindrical Li-Ion Cells. *J. Power Sources* **2014**, *252*, 298–304. [\[CrossRef\]](#)
25. Zeng, Y.; Chalise, D.; Lubner, S.D.; Kaur, S.; Prasher, R.S. A Review of Thermal Physics and Management inside Lithium-Ion Batteries for High Energy Density and Fast Charging. *Energy Storage Mater.* **2021**, *41*, 264–288. [\[CrossRef\]](#)
26. Kumar, R.; Goel, V. A Study on Thermal Management System of Lithium-Ion Batteries for Electrical Vehicles: A Critical Review. *J. Energy Storage* **2023**, *71*, 108025. [\[CrossRef\]](#)
27. Gan, Y.; Wang, J.; Liang, J.; Huang, Z.; Hu, M. Development of Thermal Equivalent Circuit Model of Heat Pipe-Based Thermal Management System for a Battery Module with Cylindrical Cells. *Appl. Therm. Eng.* **2020**, *164*, 114523. [\[CrossRef\]](#)
28. Feng, L.; Zhou, S.; Li, Y.; Wang, Y.; Zhao, Q.; Luo, C.; Wang, G.; Yan, K. Experimental Investigation of Thermal and Strain Management for Lithium-Ion Battery Pack in Heat Pipe Cooling. *J. Energy Storage* **2018**, *16*, 84–92. [\[CrossRef\]](#)
29. Liu, W.; Jia, Z.; Luo, Y.; Xie, W.; Deng, T. Experimental Investigation on Thermal Management of Cylindrical Li-Ion Battery Pack Based on Vapor Chamber Combined with Fin Structure. *Appl. Therm. Eng.* **2019**, *162*, 114272. [\[CrossRef\]](#)

30. Alihosseini, A.; Shafaei, M. Experimental Study and Numerical Simulation of a Lithium-Ion Battery Thermal Management System Using a Heat Pipe. *J. Energy Storage* **2021**, *39*, 102616. [[CrossRef](#)]
31. Wang, J.; Gan, Y.; Liang, J.; Tan, M.; Li, Y. Sensitivity Analysis of Factors Influencing a Heat Pipe-Based Thermal Management System for a Battery Module with Cylindrical Cells. *Appl. Therm. Eng.* **2019**, *151*, 475–485. [[CrossRef](#)]
32. Li, Y.; Bai, M.; Zhou, Z.; Lv, J.; Hu, C.; Gao, L.; Peng, C.; Li, Y.; Li, Y.; Song, Y. Experimental Study of Liquid Immersion Cooling for Different Cylindrical Lithium-Ion Batteries under Rapid Charging Conditions. *Therm. Sci. Eng. Prog.* **2023**, *37*, 101569. [[CrossRef](#)]
33. Liu, Y.; Aldan, G.; Huang, X.; Hao, M. Single-Phase Static Immersion Cooling for Cylindrical Lithium-Ion Battery Module. *Appl. Therm. Eng.* **2023**, *233*, 121184. [[CrossRef](#)]
34. Song, W.; Bai, F.; Chen, M.; Lin, S.; Feng, Z.; Li, Y. Thermal Management of Standby Battery for Outdoor Base Station Based on the Semiconductor Thermoelectric Device and Phase Change Materials. *Appl. Therm. Eng.* **2018**, *137*, 203–217. [[CrossRef](#)]
35. Yang, W.; Zhou, F.; Zhou, H.; Liu, Y. Thermal Performance of Axial Air Cooling System with Bionic Surface Structure for Cylindrical Lithium-Ion Battery Module. *Int. J. Heat Mass Transf.* **2020**, *161*, 120307. [[CrossRef](#)]
36. Zhou, H.; Zhou, F.; Xu, L.; Kong, J.; Yang, Q. Thermal Performance of Cylindrical Lithium-Ion Battery Thermal Management System Based on Air Distribution Pipe. *Int. J. Heat Mass Transf.* **2019**, *131*, 984–998. [[CrossRef](#)]
37. Wang, T.; Tseng, K.J.; Zhao, J.; Wei, Z. Thermal Investigation of Lithium-Ion Battery Module with Different Cell Arrangement Structures and Forced Air-Cooling Strategies. *Appl. Energy* **2014**, *134*, 229–238. [[CrossRef](#)]
38. Kummitha, O.R. Thermal Cooling of Li-Ion Cylindrical Cells Battery Module with Baffles Arrangement for Airflow Cooling Numerical Analysis. *J. Energy Storage* **2023**, *59*, 106474. [[CrossRef](#)]
39. Lu, Z.; Yu, X.; Wei, L.; Qiu, Y.; Zhang, L.; Meng, X.; Jin, L. Parametric Study of Forced Air Cooling Strategy for Lithium-Ion Battery Pack with Staggered Arrangement. *Appl. Therm. Eng.* **2018**, *136*, 28–40. [[CrossRef](#)]
40. Ji, C.; Wang, B.; Wang, S.; Pan, S.; Wang, D.; Qi, P.; Zhang, K. Optimization on Uniformity of Lithium-Ion Cylindrical Battery Module by Different Arrangement Strategy. *Appl. Therm. Eng.* **2019**, *157*, 113683. [[CrossRef](#)]
41. Koorata, P.K.; Chandrasekaran, N. Numerical Investigation of Cooling Performance of a Novel Air-Cooled Thermal Management System for Cylindrical Li-Ion Battery Module. *Appl. Therm. Eng.* **2021**, *193*, 116961. [[CrossRef](#)]
42. Lee, N.; Choi, J.; Lee, J.; Shin, D.; Um, S. Prognostic Analysis of Thermal Interface Material Effects on Anisotropic Heat Transfer Characteristics and State of Health of a 21700 Cylindrical Lithium-Ion Battery Module. *J. Energy Storage* **2023**, *72*, 108594. [[CrossRef](#)]
43. Mahamud, R.; Park, C. Reciprocating Air Flow for Li-Ion Battery Thermal Management to Improve Temperature Uniformity. *J. Power Sources* **2011**, *196*, 5685–5696. [[CrossRef](#)]
44. Wang, Y.; Liu, B.; Han, P.; Hao, C.; Li, S.; You, Z.; Wang, M. Optimization of an Air-Based Thermal Management System for Lithium-Ion Battery Packs. *J. Energy Storage* **2021**, *44*, 103314. [[CrossRef](#)]
45. Jaliliantabar, F.; Mamat, R.; Kumarasamy, S. Prediction of Lithium-Ion Battery Temperature in Different Operating Conditions Equipped with Passive Battery Thermal Management System by Artificial Neural Networks. *Mater. Today Proc.* **2022**, *48*, 1796–1804. [[CrossRef](#)]
46. Li, A.; Yuen, A.C.Y.; Wang, W.; Chen, T.B.Y.; Lai, C.S.; Yang, W.; Wu, W.; Chan, Q.N.; Kook, S.; Yeoh, G.H. Integration of Computational Fluid Dynamics and Artificial Neural Network for Optimization Design of Battery Thermal Management System. *Batteries* **2022**, *8*, 69. [[CrossRef](#)]
47. Wang, Y.; Chen, X.; Li, C.; Yu, Y.; Zhou, G.; Wang, C.Y.; Zhao, W. Temperature Prediction of Lithium-Ion Battery Based on Artificial Neural Network Model. *Appl. Therm. Eng.* **2023**, *228*, 120482. [[CrossRef](#)]
48. Gao, R.; Fan, Z.; Liu, S. A Gradient Channel-Based Novel Design of Liquid-Cooled Battery Thermal Management System for Thermal Uniformity Improvement. *J. Energy Storage* **2022**, *48*, 104014. [[CrossRef](#)]
49. Yates, M.; Akrami, M.; Javadi, A.A. Analysing the Performance of Liquid Cooling Designs in Cylindrical Lithium-Ion Batteries. *J. Energy Storage* **2021**, *33*, 100913. [[CrossRef](#)]
50. Li, W.; Garg, A.; Wang, N.; Gao, L.; Le Phung, M.L.; Tran, V.M. Computational Fluid Dynamics-Based Numerical Analysis for Studying the Effect of Mini-Channel Cooling Plate, Flow Characteristics, and Battery Arrangement for Cylindrical Lithium-Ion Battery Pack. *J. Electrochem. Energy Convers. Storage* **2022**, *19*, 041003. [[CrossRef](#)]
51. Xia, C.; Fu, J.; Lai, J.; Yao, X.; Chen, Z. Conjugate Heat Transfer in Fractal Tree-like Channels Network Heat Sink for High-Speed Motorized Spindle Cooling. *Appl. Therm. Eng.* **2015**, *90*, 1032–1042. [[CrossRef](#)]
52. Wang, H.; Tao, T.; Xu, J.; Mei, X.; Liu, X.; Gou, P. Cooling Capacity of a Novel Modular Liquid-Cooled Battery Thermal Management System for Cylindrical Lithium Ion Batteries. *Appl. Therm. Eng.* **2020**, *178*, 115591. [[CrossRef](#)]
53. Kim, B.R.; Nguyen, T.N.; Park, C.W. Cooling Performance of Thermal Management System for Lithium-Ion Batteries Using Two Types of Cold Plate: Experiment and MATLAB/Simulink-Simscape Simulation. *Int. Commun. Heat Mass Transf.* **2023**, *145*, 106816. [[CrossRef](#)]
54. Sheng, L.; Zhang, H.; Su, L.; Zhang, Z.; Zhang, H.; Li, K.; Fang, Y.; Ye, W. Effect Analysis on Thermal Profile Management of a Cylindrical Lithium-Ion Battery Utilizing a Cellular Liquid Cooling Jacket. *Energy* **2021**, *220*, 119725. [[CrossRef](#)]
55. Xu, Q.; Xie, Y.; Huang, Y.; Li, X.; Huang, H.; Bei, S.; Wang, H.; Zheng, K.; Wang, X.; Li, L. Enhancement of Thermal Management for Cylindrical Battery Module Based on a Novel Wrench-Shaped Design for the Cold Plate. *Sustain. Energy Technol. Assess.* **2023**, *59*, 103421. [[CrossRef](#)]

56. Liu, Z.; Liu, X.; Meng, H.; Guo, L.; Zhang, Z. Numerical Analysis of the Thermal Performance of a Liquid Cooling Battery Module Based on the Gradient Ratio Flow Velocity and Gradient Increment Tube Diameter. *Int. J. Heat Mass Transf.* **2021**, *175*, 121338. [[CrossRef](#)]
57. Tete, P.R.; Gupta, M.M.; Joshi, S.S. Numerical Investigation on Thermal Characteristics of a Liquid-Cooled Lithium-Ion Battery Pack with Cylindrical Cell Casings and a Square Duct. *J. Energy Storage* **2022**, *48*, 104041. [[CrossRef](#)]
58. Lai, Y.; Wu, W.; Chen, K.; Wang, S.; Xin, C. A Compact and Lightweight Liquid-Cooled Thermal Management Solution for Cylindrical Lithium-Ion Power Battery Pack. *Int. J. Heat Mass Transf.* **2019**, *144*, 118581. [[CrossRef](#)]
59. Shan, S.; Li, L.; Xu, Q.; Ling, L.; Xie, Y.; Wang, H.; Zheng, K.; Zhang, L.; Bei, S. Numerical Investigation of a Compact and Lightweight Thermal Management System with Axially Mounted Cooling Tubes for Cylindrical Lithium-Ion Battery Module. *Energy* **2023**, *274*, 127410. [[CrossRef](#)]
60. Xiong, X.; Wang, Z.; Fan, Y.; Wang, H. Numerical Analysis of Cylindrical Lithium-Ion Battery Thermal Management System Based on Bionic Flow Channel Structure. *Therm. Sci. Eng. Prog.* **2023**, *42*, 101879. [[CrossRef](#)]
61. Liang, G.; Li, J.; He, J.; Tian, J.; Chen, X.; Chen, L. Numerical Investigation on a Unitization-Based Thermal Management for Cylindrical Lithium-Ion Batteries. *Energy Rep.* **2022**, *8*, 4608–4621. [[CrossRef](#)]
62. Tousi, M.; Sarchami, A.; Kiani, M.; Najafi, M.; Houshfar, E. Numerical Study of Novel Liquid-Cooled Thermal Management System for Cylindrical Li-Ion Battery Packs under High Discharge Rate Based on AgO Nanofluid and Copper Sheath. *J. Energy Storage* **2021**, *41*, 102910. [[CrossRef](#)]
63. Sarchami, A.; Najafi, M.; Imam, A.; Houshfar, E. Experimental Study of Thermal Management System for Cylindrical Li-Ion Battery Pack Based on Nanofluid Cooling and Copper Sheath. *Int. J. Therm. Sci.* **2021**, *171*, 107244. [[CrossRef](#)]
64. Zeng, W.; Ma, C.; Hu, S.; Li, S.; Zhang, Y. The Performance Investigation and Optimization of Reciprocating Flow Applied for Liquid-Cooling-Based Battery Thermal Management System. *Energy Convers. Manag.* **2023**, *292*, 117378. [[CrossRef](#)]
65. Ma, Y.; Mou, H.; Zhao, H. Cooling Optimization Strategy for Lithium-Ion Batteries Based on Triple-Step Nonlinear Method. *Energy* **2020**, *201*, 117678. [[CrossRef](#)]
66. Wang, Y.; Zhang, G.; Yang, X. Optimization of Liquid Cooling Technology for Cylindrical Power Battery Module. *Appl. Therm. Eng.* **2019**, *162*, 114200. [[CrossRef](#)]
67. Xie, L.; Huang, Y.; Lai, H. Coupled Prediction Model of Liquid-Cooling Based Thermal Management System for Cylindrical Lithium-Ion Module. *Appl. Therm. Eng.* **2020**, *178*, 115599. [[CrossRef](#)]
68. Talele, V.; Patil, M.S.; Panchal, S.; Fraser, R.; Fowler, M.; Gunti, S.R. Novel Metallic Separator Coupled Composite Phase Change Material Passive Thermal Design for Large Format Prismatic Battery Pack. *J. Energy Storage* **2023**, *58*, 106336. [[CrossRef](#)]
69. Talele, V.; Zhao, P. Effect of Nano-Enhanced Phase Change Material on the Thermal Management of a 18650 NMC Battery Pack. *J. Energy Storage* **2023**, *64*, 107068. [[CrossRef](#)]
70. Najafi Khaboshan, H.; Jaliliantabar, F.; Adam Abdullah, A.; Panchal, S. Improving the Cooling Performance of Cylindrical Lithium-Ion Battery Using Three Passive Methods in a Battery Thermal Management System. *Appl. Therm. Eng.* **2023**, *227*, 120320. [[CrossRef](#)]
71. Sun, Z.; Fan, R.; Yan, F.; Zhou, T.; Zheng, N. Thermal Management of the Lithium-Ion Battery by the Composite PCM-Fin Structures. *Int. J. Heat Mass Transf.* **2019**, *145*, 118739. [[CrossRef](#)]
72. Chen, H.; Abidi, A.; Hussein, A.K.; Younis, O.; Degani, M.; Heidarshenas, B. Investigation of the Use of Extended Surfaces in Paraffin Wax Phase Change Material in Thermal Management of a Cylindrical Lithium-Ion Battery: Applicable in the Aerospace Industry. *J. Energy Storage* **2022**, *45*, 103685. [[CrossRef](#)]
73. Mansir, I.B.; Sinaga, N.; Farouk, N.; Aljaghtam, M.; Diyoke, C.; Nguyen, D.D. Numerical Simulation of Dimensions and Arrangement of Triangular Fins Mounted on Cylindrical Lithium-Ion Batteries in Passive Thermal Management. *J. Energy Storage* **2022**, *50*, 104392. [[CrossRef](#)]
74. Qi, X.; Sidi, M.O.; Tlili, I.; Ibrahim, T.K.; Elkotb, M.A.; El-Shorbagy, M.A.; Li, Z. Optimization and Sensitivity Analysis of Extended Surfaces during Melting and Freezing of Phase Changing Materials in Cylindrical Lithium-Ion Battery Cooling. *J. Energy Storage* **2022**, *51*, 104545. [[CrossRef](#)]
75. Zhou, Z.; Chen, S.; Luo, M.; Du, W.; Wu, Y.; Yu, Y. Effect of Mechanical Vibration on Phase Change Material Based Thermal Management System for a Cylindrical Lithium-Ion Battery at High Ambient Temperature and High Discharge Rate. *Int. J. Heat Mass Transf.* **2023**, *211*, 124255. [[CrossRef](#)]
76. El Idi, M.M.; Karkri, M.; Abdou Tankari, M. A Passive Thermal Management System of Li-Ion Batteries Using PCM Composites: Experimental and Numerical Investigations. *Int. J. Heat Mass Transf.* **2021**, *169*, 120894. [[CrossRef](#)]
77. Sazvar, B.; Moqtaderi, H. A Numerical Study on the Capacity Improvement of Cylindrical Battery Cooling Systems Using Nano-Enhanced Phase Change Material and Axisymmetric Stepped Fins. *J. Energy Storage* **2023**, *62*, 106833. [[CrossRef](#)]
78. Ranjbar Kermani, J.; Mahlouji Taheri, M.; Shafii, M.B.; Moosavi, A. Analytical Solution, Optimization and Design of a Phase Change Cooling Pack for Cylindrical Lithium-Ion Batteries. *Appl. Therm. Eng.* **2023**, *232*, 120963. [[CrossRef](#)]
79. Li, Y.; Du, Y.; Xu, T.; Wu, H.; Zhou, X.; Ling, Z.; Zhang, Z. Optimization of Thermal Management System for Li-Ion Batteries Using Phase Change Material. *Appl. Therm. Eng.* **2018**, *131*, 766–778. [[CrossRef](#)]
80. Angani, A.; Kim, H.W.; Hwang, M.H.; Kim, E.; Kim, K.M.; Cha, H.R. A Comparison between Zig-Zag Plated Hybrid Parallel Pipe and Liquid Cooling Battery Thermal Management Systems for Lithium-Ion Battery Module. *Appl. Therm. Eng.* **2023**, *219*, 119599. [[CrossRef](#)]

81. Zhou, H.; Niu, J.; Guo, X.; Xu, L.; Song, Z.; Yin, X. Thermal Performance of a Hybrid Thermal Management System Based on the Half Helical Coil Coupled with Air Jet Cooling for Cylindrical Lithium-Ion Battery. *Appl. Therm. Eng.* **2023**, *225*, 120231. [[CrossRef](#)]
82. Xin, S.; Wang, C.; Xi, H. Thermal Management Scheme and Optimization of Cylindrical Lithium-Ion Battery Pack Based on Air Cooling and Liquid Cooling. *Appl. Therm. Eng.* **2023**, *224*, 120100. [[CrossRef](#)]
83. Yang, W.; Zhou, F.; Liu, Y.; Xu, S.; Chen, X. Thermal Performance of Honeycomb-like Battery Thermal Management System with Bionic Liquid Mini-Channel and Phase Change Materials for Cylindrical Lithium-Ion Battery. *Appl. Therm. Eng.* **2021**, *188*, 116649. [[CrossRef](#)]
84. Al-Rashed, A.A.A. Thermal Management of Lithium-Ion Batteries with Simultaneous Use of Hybrid Nanofluid and Nano-Enhanced Phase Change Material: A Numerical Study. *J. Energy Storage* **2022**, *46*, 103730. [[CrossRef](#)]
85. Xin, Q.; Xiao, J.; Yang, T.; Zhang, H.; Long, X. Thermal Management of Lithium-Ion Batteries under High Ambient Temperature and Rapid Discharging Using Composite PCM and Liquid Cooling. *Appl. Therm. Eng.* **2022**, *210*, 118230. [[CrossRef](#)]
86. Cao, J.; Luo, M.; Fang, X.; Ling, Z.; Zhang, Z. Liquid Cooling with Phase Change Materials for Cylindrical Li-Ion Batteries: An Experimental and Numerical Study. *Energy* **2020**, *191*, 116565. [[CrossRef](#)]
87. An, Z.; Chen, X.; Zhao, L.; Gao, Z. Numerical Investigation on Integrated Thermal Management for a Lithium-Ion Battery Module with a Composite Phase Change Material and Liquid Cooling. *Appl. Therm. Eng.* **2019**, *163*, 114345. [[CrossRef](#)]
88. Zeng, W.; Niu, Y.; Li, S.; Hu, S.; Mao, B.; Zhang, Y. Cooling Performance and Optimization of a New Hybrid Thermal Management System of Cylindrical Battery. *Appl. Therm. Eng.* **2022**, *217*, 119171. [[CrossRef](#)]
89. Peng, P.; Wang, Y.; Jiang, F. Numerical Study of PCM Thermal Behavior of a Novel PCM-Heat Pipe Combined System for Li-Ion Battery Thermal Management. *Appl. Therm. Eng.* **2022**, *209*, 118293. [[CrossRef](#)]
90. Zhou, J.; Zhang, S.; Yang, H.; Dong, F. Thermal Performance of a Novel Honeycomb Cooling System for Cylindrical Lithium-Ion Batteries. *Heat Transf. Eng.* **2023**, 1–17. [[CrossRef](#)]
91. Hasan, H.A.; Togun, H.; Abed, A.M.; Biswas, N.; Mohammed, H.I. Thermal Performance Assessment for an Array of Cylindrical Lithium-Ion Battery Cells Using an Air-Cooling System. *Appl. Energy* **2023**, *346*, 121354. [[CrossRef](#)]
92. Zhao, J.; Rao, Z.; Huo, Y.; Liu, X.; Li, Y. Thermal Management of Cylindrical Power Battery Module for Extending the Life of New Energy Electric Vehicles. *Appl. Therm. Eng.* **2015**, *85*, 33–43. [[CrossRef](#)]
93. Li, X.; He, F.; Ma, L. Thermal Management of Cylindrical Batteries Investigated Using Wind Tunnel Testing and Computational Fluid Dynamics Simulation. *J. Power Sources* **2013**, *238*, 395–402. [[CrossRef](#)]
94. Hai, T.; Abidi, A.; Sajadi, S.M.; Zain, J.M.; Malekshah, E.H.; Aybar, H. Simultaneous Cooling of Plate and Cylindrical Batteries in an Air-Cooled Lithium Battery Thermal Management System, by Changing the Distances of the Batteries from Each Other and the Pack Wall. *J. Taiwan Inst. Chem. Eng.* **2023**, *148*, 104931. [[CrossRef](#)]
95. Li, S.; Kirkaldy, N.; Zhang, C.; Gopalakrishnan, K.; Amietszajew, T.; Diaz, L.B.; Barreras, J.V.; Shams, M.; Hua, X.; Patel, Y.; et al. Optimal Cell Tab Design and Cooling Strategy for Cylindrical Lithium-Ion Batteries. *J. Power Sources* **2021**, *492*, 229594. [[CrossRef](#)]
96. Saechan, P.; Dhuchakallaya, I. Numerical Study on the Air-Cooled Thermal Management of Lithium-Ion Battery Pack for Electrical Vehicles. *Energy Rep.* **2022**, *8*, 1264–1270. [[CrossRef](#)]
97. Ruhani, B.; Abidi, A.; Hussein, A.K.; Younis, O.; Degani, M.; Sharifpur, M. Numerical Simulation of the Effect of Battery Distance and Inlet and Outlet Length on the Cooling of Cylindrical Lithium-Ion Batteries and Overall Performance of Thermal Management System. *J. Energy Storage* **2022**, *45*, 103714. [[CrossRef](#)]
98. Xun, J.; Liu, R.; Jiao, K. Numerical and Analytical Modeling of Lithium Ion Battery Thermal Behaviors with Different Cooling Designs. *J. Power Sources* **2013**, *233*, 47–61. [[CrossRef](#)]
99. Zhao, C.; Sousa, A.C.M.; Jiang, F. Minimization of Thermal Non-Uniformity in Lithium-Ion Battery Pack Cooled by Channeled Liquid Flow. *Int. J. Heat Mass Transf.* **2019**, *129*, 660–670. [[CrossRef](#)]
100. Yang, T.; Yang, N.; Zhang, X.; Li, G. Investigation of the Thermal Performance of Axial-Flow Air Cooling for the Lithium-Ion Battery Pack. *Int. J. Therm. Sci.* **2016**, *108*, 132–144. [[CrossRef](#)]
101. Fan, Y.; Bao, Y.; Ling, C.; Chu, Y.; Tan, X.; Yang, S. Experimental Study on the Thermal Management Performance of Air Cooling for High Energy Density Cylindrical Lithium-Ion Batteries. *Appl. Therm. Eng.* **2019**, *155*, 96–109. [[CrossRef](#)]
102. Cen, J.; Li, Z.; Jiang, F. Experimental Investigation on Using the Electric Vehicle Air Conditioning System for Lithium-Ion Battery Thermal Management. *Energy Sustain. Dev.* **2018**, *45*, 88–95. [[CrossRef](#)]
103. Jiaqiang, E.; Yue, M.; Chen, J.; Zhu, H.; Deng, Y.; Zhu, Y.; Zhang, F.; Wen, M.; Zhang, B.; Kang, S. Effects of the Different Air Cooling Strategies on Cooling Performance of a Lithium-Ion Battery Module with Baffle. *Appl. Therm. Eng.* **2018**, *144*, 231–241. [[CrossRef](#)]
104. Chen, H.; Abidi, A.; Mohammad Sajadi, S.; Yuan, Y.; Aybar, H.; Heidarshenas, B. Effect of Splitter Damper on Airflow Conduction for Thermal Management of a Lithium-Ion Battery Cooling System with Plate and Cylindrical Batteries. *J. Taiwan Inst. Chem. Eng.* **2023**, *148*, 104853. [[CrossRef](#)]
105. Hai, T.; Said, N.M.; Cheraghian, G.; Zhou, J.; Malekshah, E.H.; Sharifpur, M. Effect of Air Inlet and Outlet Cross Sections on the Cooling System of Cylindrical Lithium Battery with Segmental Arrangement Utilized in Electric Vehicles. *J. Power Sources* **2023**, *553*, 232222. [[CrossRef](#)]
106. Wang, T.; Tseng, K.J.; Zhao, J. Development of Efficient Air-Cooling Strategies for Lithium-Ion Battery Module Based on Empirical Heat Source Model. *Appl. Therm. Eng.* **2015**, *90*, 521–529. [[CrossRef](#)]

107. Shahid, S.; Agelin-Chaab, M. Development and Analysis of a Technique to Improve Air-Cooling and Temperature Uniformity in a Battery Pack for Cylindrical Batteries. *Therm. Sci. Eng. Prog.* **2018**, *5*, 351–363. [[CrossRef](#)]
108. Zhang, F.; Wang, P.; Yi, M. Design Optimization of Forced Air-Cooled Lithium-Ion Battery Module Based on Multi-Vents. *J. Energy Storage* **2021**, *40*, 102781. [[CrossRef](#)]
109. Hasan, H.A.; Togun, H.; Mohammed, H.I.; Abed, A.M.; Homod, R.Z. CFD Simulation of Effect Spacing between Lithium-Ion Batteries by Using Flow Air inside the Cooling Pack. *J. Energy Storage* **2023**, *72*, 108631. [[CrossRef](#)]
110. Yang, N.; Zhang, X.; Li, G.; Hua, D. Assessment of the Forced Air-Cooling Performance for Cylindrical Lithium-Ion Battery Packs: A Comparative Analysis between Aligned and Staggered Cell Arrangements. *Appl. Therm. Eng.* **2015**, *80*, 55–65. [[CrossRef](#)]
111. Shahid, S.; Agelin-Chaab, M. Analysis of Cooling Effectiveness and Temperature Uniformity in a Battery Pack for Cylindrical Batteries. *Energies* **2017**, *10*, 1157. [[CrossRef](#)]
112. Peng, X.; Cui, X.; Liao, X.; Garg, A. A Thermal Investigation and Optimization of an Air-Cooled Lithium-Ion Battery Pack. *Energies* **2020**, *13*, 2956. [[CrossRef](#)]
113. Hai, T.; Abidi, A.; Abed, A.M.; Zhou, J.; Malekshah, E.H.; Aybar, H. Three-Dimensional Numerical Study of the Effect of an Air-Cooled System on Thermal Management of a Cylindrical Lithium-Ion Battery Pack with Two Different Arrangements of Battery Cells. *J. Power Sources* **2022**, *550*, 232117. [[CrossRef](#)]
114. Reyes-Marambio, J.; Moser, F.; Gana, F.; Severino, B.; Calderón-Muñoz, W.R.; Palma-Behnke, R.; Estevez, P.A.; Orchard, M.; Cortés, M. A Fractal Time Thermal Model for Predicting the Surface Temperature of Air-Cooled Cylindrical Li-Ion Cells Based on Experimental Measurements. *J. Power Sources* **2016**, *306*, 636–645. [[CrossRef](#)]
115. Qin, P.; Liao, M.; Mei, W.; Sun, J.; Wang, Q. The Experimental and Numerical Investigation on a Hybrid Battery Thermal Management System Based on Forced-Air Convection and Internal Finned Structure. *Appl. Therm. Eng.* **2021**, *195*, 117212. [[CrossRef](#)]
116. Saw, L.H.; Ye, Y.; Tay, A.A.O.; Chong, W.T.; Kuan, S.H.; Yew, M.C. Computational Fluid Dynamic and Thermal Analysis of Lithium-Ion Battery Pack with Air Cooling. *Appl. Energy* **2016**, *177*, 783–792. [[CrossRef](#)]
117. Yu, X.; Lu, Z.; Zhang, L.; Wei, L.; Cui, X.; Jin, L. Experimental Study on Transient Thermal Characteristics of Stagger-Arranged Lithium-Ion Battery Pack with Air Cooling Strategy. *Int. J. Heat Mass Transf.* **2019**, *143*, 118576. [[CrossRef](#)]
118. Wang, Y.W.; Jiang, J.M.; Chung, Y.H.; Chen, W.C.; Shu, C.M. Forced-Air Cooling System for Large-Scale Lithium-Ion Battery Modules during Charge and Discharge Processes. *J. Therm. Anal. Calorim.* **2019**, *135*, 2891–2901. [[CrossRef](#)]
119. Sun, Y.; Bai, R.; Ma, J. Development and Analysis of a New Cylindrical Lithium-Ion Battery Thermal Management System. *Chin. J. Mech. Eng.* **2022**, *35*, 1–15. [[CrossRef](#)]
120. Chang, G.; Cui, X.; Li, Y.; Ji, Y. Effects of Reciprocating Liquid Flow Battery Thermal Management System on Thermal Characteristics and Uniformity of Large Lithium-Ion Battery Pack. *Int. J. Energy Res.* **2020**, *44*, 6383–6395. [[CrossRef](#)]
121. Dong, F.; Cheng, Z.; Zhu, J.; Song, D.; Ni, J. Investigation and Optimization on Cooling Performance of a Novel Double Helix Structure for Cylindrical Lithium-Ion Batteries. *Appl. Therm. Eng.* **2021**, *189*, 116758. [[CrossRef](#)]
122. Li, W.; Garg, A.; Xiao, M.; Gao, L. Optimization for Liquid Cooling Cylindrical Battery Thermal Management System Based on Gaussian Process Model. *Therm. Sci. Eng. Appl.* **2021**, *13*, 021015. [[CrossRef](#)]
123. Liu, Z.; Wang, H.; Yang, C.; Zhao, J. Simulation Study of Lithium-Ion Battery Thermal Management System Based on a Variable Flow Velocity Method with Liquid Metal. *Appl. Therm. Eng.* **2020**, *179*, 115578. [[CrossRef](#)]
124. Yao, F.; Guan, X.; Yang, M.; Wen, C. Study on Liquid Cooling Heat Dissipation of Li-Ion Battery Pack Based on Bionic Cobweb Channel. *J. Energy Storage* **2023**, *68*, 107588. [[CrossRef](#)]
125. Zhao, C.; Cao, W.; Dong, T.; Jiang, F. Thermal Behavior Study of Discharging/Charging Cylindrical Lithium-Ion Battery Module Cooled by Channeled Liquid Flow. *Int. J. Heat Mass Transf.* **2018**, *120*, 751–762. [[CrossRef](#)]
126. Esmaeili, Z.; Khoshvaght-Aliabadi, M. Thermal Management and Temperature Uniformity Enhancement of Cylindrical Lithium-Ion Battery Pack Based on Liquid Cooling Equipped with Twisted Tapes. *J. Taiwan Inst. Chem. Eng.* **2023**, *148*, 104671. [[CrossRef](#)]
127. Zhou, H.; Zhou, F.; Zhang, Q.; Wang, Q.; Song, Z. Thermal Management of Cylindrical Lithium-Ion Battery Based on a Liquid Cooling Method with Half-Helical Duct. *Appl. Therm. Eng.* **2019**, *162*, 114257. [[CrossRef](#)]
128. Rao, Z.; Qian, Z.; Kuang, Y.; Li, Y. Thermal Performance of Liquid Cooling Based Thermal Management System for Cylindrical Lithium-Ion Battery Module with Variable Contact Surface. *Appl. Therm. Eng.* **2017**, *123*, 1514–1522. [[CrossRef](#)]
129. Zhao, J.; Rao, Z.; Li, Y. Thermal Performance of Mini-Channel Liquid Cooled Cylinder Based Battery Thermal Management for Cylindrical Lithium-Ion Power Battery. *Energy Convers. Manag.* **2015**, *103*, 157–165. [[CrossRef](#)]
130. Huang, Y.; Wang, S.; Lu, Y.; Huang, R.; Yu, X. Study on a Liquid Cooled Battery Thermal Management System Pertaining to the Transient Regime. *Appl. Therm. Eng.* **2020**, *180*, 115793. [[CrossRef](#)]
131. Hasan, H.A.; Togun, H.; Abed, A.M.; Qasem, N.A.A.; Abderrahmane, A.; Guedri, K.; Eldin, S.M. Numerical Investigation on Cooling Cylindrical Lithium-Ion-Battery by Using Different Types of Nanofluids in an Innovative Cooling System. *Case Stud. Therm. Eng.* **2023**, *49*, 103097. [[CrossRef](#)]
132. Bohacek, J.; Raudensky, M.; Karimi-Sibaki, E. Polymeric Hollow Fibers: Uniform Temperature of Li-Ion Cells in Battery Modules. *Appl. Therm. Eng.* **2019**, *159*, 113940. [[CrossRef](#)]
133. Lv, Y.; Zhou, D.; Yang, X.; Liu, X.; Li, X.; Zhang, G. Experimental Investigation on a Novel Liquid-Cooling Strategy by Coupling with Graphene-Modified Silica Gel for the Thermal Management of Cylindrical Battery. *Appl. Therm. Eng.* **2019**, *159*, 113885. [[CrossRef](#)]

134. An, Z.; Li, D.; Zhang, C.; Luo, Y.; Zhang, J. Behaviours of Thermal Management System with Micro Channels for Cylindrical Lithium-Ion Cells under Fuzzy-PID Control Strategy. *Appl. Therm. Eng.* **2023**, *233*, 121089. [[CrossRef](#)]
135. Lamrani, B.; Lebrouhi, B.E.; Khattari, Y.; Kousksou, T. A Simplified Thermal Model for a Lithium-Ion Battery Pack with Phase Change Material Thermal Management System. *J. Energy Storage* **2021**, *44*, 103377. [[CrossRef](#)]
136. Karimi, G.; Azizi, M.; Babapoor, A. Experimental Study of a Cylindrical Lithium Ion Battery Thermal Management Using Phase Change Material Composites. *J. Energy Storage* **2016**, *8*, 168–174. [[CrossRef](#)]
137. Lv, Y.; Yang, X.; Li, X.; Zhang, G.; Wang, Z.; Yang, C. Experimental Study on a Novel Battery Thermal Management Technology Based on Low Density Polyethylene-Enhanced Composite Phase Change Materials Coupled with Low Fins. *Appl. Energy* **2016**, *178*, 376–382. [[CrossRef](#)]
138. Bais, A.R.; Subhedhar, D.G.; Joshi, N.C.; Panchal, S. Numerical Investigation on Thermal Management System for Lithium Ion Battery Using Phase Change Material. *Mater. Today Proc.* **2022**, *66*, 1726–1733. [[CrossRef](#)]
139. Liu, J.; Ma, Q.; Li, X. Numerical Simulation of the Combination of Novel Spiral Fin and Phase Change Material for Cylindrical Lithium-Ion Batteries in Passive Thermal Management. *Energies* **2022**, *15*, 8847. [[CrossRef](#)]
140. Wang, Z.; Liu, Y.; Mahmoud, M.Z. Simultaneous Application of Active and Passive Methods in Cooling of a Cylindrical Lithium-Ion Battery by Changing the Size of the Elliptical Cavity Filled with Nano Phase Change Materials. *J. Energy Storage* **2022**, *50*, 104693. [[CrossRef](#)]
141. Wang, S.; Li, Y.; Li, Y.Z.; Mao, Y.; Zhang, Y.; Guo, W.; Zhong, M. A Forced Gas Cooling Circle Packaging with Liquid Cooling Plate for the Thermal Management of Li-Ion Batteries under Space Environment. *Appl. Therm. Eng.* **2017**, *123*, 929–939. [[CrossRef](#)]
142. Chen, X.; Zhou, F.; Yang, W.; Gui, Y.; Zhang, Y. A Hybrid Thermal Management System with Liquid Cooling and Composite Phase Change Materials Containing Various Expanded Graphite Contents for Cylindrical Lithium-Ion Batteries. *Appl. Therm. Eng.* **2022**, *200*, 117702. [[CrossRef](#)]
143. Behi, H.; Karimi, D.; Behi, M.; Ghanbarpour, M.; Jaguefont, J.; Sokkeh, M.A.; Gandoman, F.H.; Berecibar, M.; Van Mierlo, J. A New Concept of Thermal Management System in Li-Ion Battery Using Air Cooling and Heat Pipe for Electric Vehicles. *Appl. Therm. Eng.* **2020**, *174*, 115280. [[CrossRef](#)]
144. Kong, D.; Peng, R.; Ping, P.; Du, J.; Chen, G.; Wen, J. A Novel Battery Thermal Management System Coupling with PCM and Optimized Controllable Liquid Cooling for Different Ambient Temperatures. *Energy Convers. Manag.* **2020**, *204*, 112280. [[CrossRef](#)]
145. Jiang, Y.; Wang, X.; Mahmoud, M.Z.; Elkotb, M.A.; Baloo, L.; Li, Z.; Heidarshenas, B. A Study of Nanoparticle Shape in Water/Alumina/Boehmite Nanofluid Flow in the Thermal Management of a Lithium-Ion Battery under the Presence of Phase-Change Materials. *J. Power Sources* **2022**, *539*, 231522. [[CrossRef](#)]
146. Khan, M.N.; Dhahad, H.A.; Alamri, S.; Anqi, A.E.; Sharma, K.; Mehrez, S.; Shamseldin, M.A.; Ibrahim, B.F. Air Cooled Lithium-Ion Battery with Cylindrical Cell in Phase Change Material Filled Cavity of Different Shapes. *J. Energy Storage* **2022**, *50*, 104573. [[CrossRef](#)]
147. Jilte, R.; Afzal, A.; Ağbulut, Ü.; Shaik, S.; Khan, S.A.; Linul, E.; Asif, M. Battery Thermal Management of a Novel Helical Channeled Cylindrical Li-Ion Battery with Nanofluid and Hybrid Nanoparticle-Enhanced Phase Change Material. *Int. J. Heat Mass Transf.* **2023**, *216*, 124547. [[CrossRef](#)]
148. Almeahmadi, F.A.; Alqaed, S.; Mustafa, J.; Jamil, B.; Sharifpur, M.; Cheraghian, G. Combining an Active Method and a Passive Method in Cooling Lithium-Ion Batteries and Using the Generated Heat in Heating a Residential Unit. *J. Energy Storage* **2022**, *49*, 104181. [[CrossRef](#)]
149. Mashayekhi, M.; Houshfar, E.; Ashjaee, M. Development of Hybrid Cooling Method with PCM and Al₂O₃ Nanofluid in Aluminium Minichannels Using Heat Source Model of Li-Ion Batteries. *Appl. Therm. Eng.* **2020**, *178*, 115543. [[CrossRef](#)]
150. Tian, M.W.; Abed, A.M.; Yan, S.R.; Sajadi, S.M.; Mahmoud, M.Z.; Aybar, H.; Smaism, G.F. Economic Cost and Numerical Evaluation of Cooling of a Cylindrical Lithium-Ion Battery Pack Using Air and Phase Change Materials. *J. Energy Storage* **2022**, *52*, 104925. [[CrossRef](#)]
151. Zadeh, P.G.; Gholamalizadeh, E.; Wang, Y.; Chung, J.D. Electrochemical Modeling of a Thermal Management System for Cylindrical Lithium-Ion Battery Pack Considering Battery Capacity Fade. *Case Stud. Therm. Eng.* **2022**, *32*, 101878. [[CrossRef](#)]
152. Shahid, S.; Agelin-Chaab, M. Experimental and Numerical Analysis of a Hybrid Thermal Management Concept at Different Discharge Rates for a Cylindrical Li-Ion Battery Module. *Batteries* **2023**, *9*, 474. [[CrossRef](#)]
153. Wang, Y.; Peng, P.; Cao, W.; Dong, T.; Zheng, Y.; Lei, B.; Shi, Y.; Jiang, F. Experimental Study on a Novel Compact Cooling System for Cylindrical Lithium-Ion Battery Module. *Appl. Therm. Eng.* **2020**, *180*, 115772. [[CrossRef](#)]
154. Zhao, J.; Lv, P.; Rao, Z. Experimental Study on the Thermal Management Performance of Phase Change Material Coupled with Heat Pipe for Cylindrical Power Battery Pack. *Exp. Therm. Fluid Sci.* **2017**, *82*, 182–188. [[CrossRef](#)]
155. Weng, J.; He, Y.; Ouyang, D.; Yang, X.; Chen, M.; Cui, S.; Zhang, G.; Yuen, R.K.K.; Wang, J. Honeycomb-Inspired Design of a Thermal Management Module and Its Mitigation Effect on Thermal Runaway Propagation. *Appl. Therm. Eng.* **2021**, *195*, 117147. [[CrossRef](#)]
156. Faizan, M.; Pati, S.; Randive, P. Implications of Novel Cold Plate Design with Hybrid Cooling on Thermal Management of Fast Discharging Lithium-Ion Battery. *J. Energy Storage* **2022**, *53*, 105051. [[CrossRef](#)]
157. Chavan, U.; Prajapati, O.; Hujare, P. Lithium Ion Battery Thermal Management by Using Coupled Heat Pipe and Liquid Cold Plate. *Mater. Today Proc.* **2023**, *80*, 382–388. [[CrossRef](#)]

158. Zhao, R.; Gu, J.; Liu, J. Optimization of a Phase Change Material Based Internal Cooling System for Cylindrical Li-Ion Battery Pack and a Hybrid Cooling Design. *Energy* **2017**, *135*, 811–822. [[CrossRef](#)]
159. Li, M.; Liu, F.; Han, B.; Guo, J.; Xu, Y. Research on Temperature Control Performance of Battery Thermal Management System Compositised with Multi-Channel Parallel Liquid Cooling and Air Cooling. *Ionics* **2021**, *27*, 2685–2695. [[CrossRef](#)]
160. Bamdezh, M.A.; Molaeimanesh, G.R.; Zanganeh, S. Role of Foam Anisotropy Used in the Phase-Change Composite Material for the Hybrid Thermal Management System of Lithium-Ion Battery. *J. Energy Storage* **2020**, *32*, 101778. [[CrossRef](#)]
161. Jiang, Y.; Smaism, G.F.; Mahmoud, M.Z.; Li, Z.; Aybar, H.; Abed, A.M. Simultaneous Numerical Investigation of the Passive Use of Phase-Change Materials and the Active Use of a Nanofluid inside a Rectangular Duct in the Thermal Management of Lithium-Ion Batteries. *J. Power Sources* **2022**, *541*, 231610. [[CrossRef](#)]
162. Qi, X.; Sajadi, S.M.; Mahmoud, M.Z.; Li, Z.; Shamseldin, M.A.; Aybar, H. Study of Circular, Horizontal and Vertical Elliptical Enclosures Filled with Phase Change Material in Thermal Management of Lithium-Ion Batteries in an Air-Cooled System. *J. Energy Storage* **2022**, *53*, 105041. [[CrossRef](#)]
163. Lee, J.; Abidi, A.; Mohammad Sajadi, S.; El-Shafay, A.S.; Degani, M.; Sharifpur, M. Study of the Effect of the Aspect Ratio of a Cylindrical Lithium-Ion Battery Enclosure in an Air-Cooled Thermal Management System. *J. Energy Storage* **2022**, *45*, 103684. [[CrossRef](#)]
164. Akkurt, N.; Aghakhani, S.; Mahmoud, M.Z.; Tag El Din, E.S.M. The Influence of Battery Distance on a Hybrid Air-Cooled Cylindrical Lithium-Ion Battery Phase Change Material Thermal Management System for Storing Solar Energy. *J. Energy Storage* **2022**, *52*, 104873. [[CrossRef](#)]
165. Cao, J.; Ling, Z.; Fang, X.; Zhang, Z. Delayed Liquid Cooling Strategy with Phase Change Material to Achieve High Temperature Uniformity of Li-Ion Battery under High-Rate Discharge. *J. Power Sources* **2020**, *450*, 227673. [[CrossRef](#)]
166. Li, J.; Zhang, H. Thermal Characteristics of Power Battery Module with Composite Phase Change Material and External Liquid Cooling. *Int. J. Heat Mass Transf.* **2020**, *156*, 119820. [[CrossRef](#)]

Disclaimer/Publisher’s Note: The statements, opinions and data contained in all publications are solely those of the individual author(s) and contributor(s) and not of MDPI and/or the editor(s). MDPI and/or the editor(s) disclaim responsibility for any injury to people or property resulting from any ideas, methods, instructions or products referred to in the content.